3. Infrared imaging/thermography

243. "Physical aspects of infrared imaging," C. H. Jones, in *The Physics of Medical Imaging,* edited by S. Webb (Adam Hilger, Bristol, 1988), pp. 488–508. (I)

4. Diaphonography/transillumination

244. "Imaging by diaphanography," S. Webb, in *The Physics of Medical Imaging,* edited by S. Webb (Adam Hilger, Bristol, 1988). pp. 524–533. (I)

245. "Transillumination imaging performance: a time-of-flight imaging system," J. C. Hebden and R. A. Kruger, Med. Phys. **17**, 351–356 (1990). (I)

ACKNOWLEDGMENTS

The author would like to acknowledge the following individuals for their assistance in preparing this Resource Letter: R. Mark Henkelman, Russell K. Hobbie, Paul C. Mangelsdorf Jr, Michael K. O'Connor, Norbert J. Pelc, James A. Sorenson, Roger H. Stuewer, and Gregg E. Trahey.

Maxwell's theory of eddy currents in thin conducting sheets, and applications to electromagnetic shielding and MAGLEV

W. M. Saslow
Department of Physics and Center for Theoretical Physics, Texas A&M University, College Station, Texas 77843-4242

(Received 1 October 1990; accepted 15 October 1991)

Using the example of a monopole that is spontaneously generated above a thin conducting sheet, the simplicity and power of Maxwell's 1872 theory of eddy currents in thin conducting sheets is illustrated. This theory employs a receding image construction, with a characteristic recession velocity $v_0=2/(\mu_0\sigma d)$, where the sheet has conductivity σ and thickness d. A modern derivation of the theory, employing the magnetic scalar potential, is also presented, with explicit use of the uniqueness theorem. Also discussed are limitations on the theory of which Maxwell, living in a time before the discovery of the electron, could not have been aware. Previous derivations either have not appealed explicitly to the uniqueness theorem, or have employed the now unfamiliar current function, and are therefore either incomplete or inaccessible to the modern reader. After the derivation, two important examples considered by Maxwell are presented—a monopole moving above a thin conducting sheet, and a monopole above a rotating thin conducting sheet (Arago's disk)—and it is argued that the lift force thus obtained makes Maxwell the grandfather, if not the father, of eddy current MAGLEV transportation systems. An energy conservation argument is given to derive Davis's result that, for a magnet of arbitrary size and shape moving parallel to a thin conducting sheet at a characteristic height h, with velocity v, the ratio of drag force to lift force is equal to v_0/v, provided that $d \ll \delta_c$, where $\delta_c = \sqrt{2h/(\mu_0\sigma v)}$. If $d \gg \delta_c$, the eddy currents are confined to a thickness δ_c, leading to an increase in the dissipation and the drag by a factor of d/δ_c, so that the ratio of drag to lift force becomes proportional to $\sqrt{v_0'/v}$, where $v_0' = 2/(\mu_0\sigma h)$. The case of a monopole fixed in position, but oscillating in strength (such as can be simulated by one end of a long, narrow, ac solenoid), is also treated. This is employed to obtain the results for an oscillating magnetic dipole whose moment is normal to the sheet. A general discussion of electromagnetic induction and electrical conductors, both thick and thin, is given, emphasizing the difference between the high-frequency limit, where flux expulsion occurs and the self-inductance dominates, and the low-frequency limit, where the flux penetrates and the electrical resistance dominates. A discussion of Lenz's law, as a statement about motion, is given. It is argued that the most general form of such a statement of Lenz's law is that induced currents tend to accelerate a conductor in the direction that most effectively decreases the rate of Joule heating. A calculation, in the low-frequency limit, of the drag force on a magnetic dipole falling down a long conducting tube, is also given. This last case can be given a striking demonstration with the newly available neodymium–iron–boron magnets.

I. INTRODUCTION

Having firmly established his inability to give adequate answers to lower division questions on eddy currents (question 12 in Chap. 35 of Ref. 1, dealing with the instantaneous and ac electromagnetic shielding by a thin conducting sheet), the author resolved to learn something of this subject in order to use it in a graduate course in Electricity and Magnetism, despite the fact that such topics receive limited or no discussion in most contemporary textbooks. The author began by reading Smythe's discussion of eddy currents.[2] There he became acquainted with a simply stated and powerful theory due to Maxwell, for eddy currents induced in thin conducting sheets. From Smythe, the author was drawn to the classic treatise by Maxwell himself,[3] and from there to Maxwell's original paper of 1872.[4] Of the discussions that the author has seen, Jeans has given the most careful derivation.[5] Jeans has also worked on a generalization of Maxwell's theory to finite sheets.[6] The author has employed the formalism to describe the eddy currents that occur on the spontaneous appearance of a magnet, or the sudden energizing of an equivalent solenoid, above a thin conducting sheet,[7] thereby answering to his satisfaction part of the lower division question posed in Ref. 1.

Before using a theory, it is important to believe in its essential correctness. Coming from Maxwell is one sort of assurance, but there should also be the sort that is internal: the theory should be derived clearly. However, the author found the derivations in Maxwell and Smythe unsatisfying, in part because they do not prove the uniqueness of the solution obtained by the image method, in part because they do not make any connection to modern formulations of the electromagnetic properties of metals, and in part because they do not give an adequate discussion of the limitations of the theory. Readers familiar with the nineteenth century formalisms of the current function and of the scalar magnetic potential for current sheets should be satisfied, on the first account, with the derivation given by Jeans. However, Jeans works out no examples, perhaps under the assumption that the reader can obtain them from a copy of Maxwell. Moreover, Jeans does not discuss the limitations of the theory. The author surmises that the theory has not made its way into contemporary textbooks because no single reference gives both examples and a convincing, modern, derivation. It is the primary purpose of the present article to provide these. Three monopole examples—spontaneous generation, oscillating strength, and uniform motion parallel to the sheet—provide a broad range of examples of eddy current shielding. (In a given source-free region, all magnetic fields can be produced by a superposition of the fields due to some set of monopoles, provided that the region is simply connected—that is, all contours drawn in it can be continuously shrunk to a point without crossing a field source.) Moreover, the derivation clarifies the limitations of the theory, limitations of which Maxwell himself, living in a time before the electromagnetic properties of metals were well understood—indeed, before the discovery of the electron—could not have been aware.

We hope to convince the reader that this subject is worthy of incorporation into the undergraduate and graduate curriculum. A by-product of such incorporation would be a better appreciation by the physics community of superconductivity as perfect diamagnetism (magnetic flux exclusion) and a better appreciation for the physical mechanism by which eddy current MAGLEV (magnetic levitation) transportation systems operate. In the author's opinion, this fundamental paper by Maxwell, Ref. 4, marks him as, if not the father, then the grandfather, of eddy current MAGLEV transportation systems.

For those with limited time: to obtain the flavor of Maxwell's theory of eddy currents, and instant expertise in the theory of MAGLEV, it is recommended that one read Sec. II, which presents the receding image construction, and Secs. VI A and B, which apply it to the calculation of lift and drag. Section VIII, which is not based on this construction, is also recommended. It utilizes nearly everything (Coulomb's law, the Biot–Savart law, Faraday's law, Ohm's law) that is taught in a first-year calculus-based course on Electricity and Magnetism to find the eddy current drag force on a magnet slowly falling through a conducting tube.

We now summarize the remainder of the paper.

Section II illustrates the idea behind Maxwell's receding image construction by considering the spontaneous generation of a monopole above a thin conducting sheet and its shielding by eddy currents. (Throughout this paper, we employ the word "shielding" exclusively to refer to electromagnetic shielding of magnetic fields by electric currents, and the word "screening" exclusively to refer to electrostatic screening of electric fields by electric charge.) The general properties of the receding image construction, using the magnetic scalar potential approach, are given in Sec. III, as well as a discussion of some general properties of the potential due to the currents induced on the surface. A derivation of the boundary condition satisfied by the magnetic field due to surface currents induced on a thin planar conductor is given in Sec. IV, and it is shown how the uniqueness theorem of electrostatics can be invoked to show that the field and the magnetic potential it can be derived from are unique. Since the receding image construction satisfies the same conditions as the potential due to the surface current, the two must be the same. Some limitations of the theory, and the fact that these limitations are different according to whether or not the system supports plasma oscillations ("good" versus "poor" conductors), are discussed.

Section V, contains an application of the theory to electromagnetic shielding—the force on a monopole, fixed in position but with pole strength oscillating in time. The oscillating dipole, a subject of more experimental relevance, is also discussed. Section VI contains a discussion of the eddy current drag and lift forces for two examples considered by Maxwell—a monopole moving above a sheet, and a monopole moving above a rotating disk. A simple derivation is then given of an important relationship between the drag and lift forces on an arbitrary magnet moving at a constant velocity parallel to a thin conducting sheet. A knowledge of the high-velocity lift force and the low-velocity drag force then permits an interpolation to be made over the entire velocity range. The drag effect, it should be noted, is relevant to an historically important phenomenon, a precursor to the discovery of Faraday's law referred to by Maxwell as "Arago's disk"; the lift effect, which Arago did *not* observe, contains the germ of eddy current MAGLEV transportation systems. Maxwell notes that, for the rotating disk geometry, there is also a radial force (whose direction can be obtained by use of the most

general form of Lenz's law, as a statement about motion, discussed in Sec. VII B).

Section VII contains a general discussion of electromagnetic shielding. In Sec. VII A we present an analysis of the field-diffusion equation, in both the low and high-frequency limits. For low frequencies the magnetic flux completely penetrates, so (using circuit terminology) electrical resistance effects dominate self-inductance effects, whereas for high frequencies the magnetic flux is expelled, so self-inductance effects dominate electrical resistance effects. In Sec. VII B we discuss Lenz's law, first observing that Lenz's law was originally intended to deal only with induced current forces that literally oppose the relative motion of a conductor and a source of magnetic field; more precisely, it was intended to describe forces due to induced currents that are linear in the velocity. We then argue that the most general form of Lenz's law is that *induced currents tend to accelerate a conductor in the direction that most effectively decreases the rate of Joule heating,* a statement that also includes effects higher order in the velocity. In applying Lenz's law it is important to observe that low velocities correspond to low frequencies, whereas high velocities correspond to high frequencies. In Sec. VII C we discuss the different behavior of both thick and thin conductors, pointing out that thin conductors have a special "semihigh" frequency regime where flux is expelled—even though the electromagnetic skin depth is much larger than the thickness—and the dissipation is much less than for a bulk material. In Sec. VII D we discuss the general issue of electromagnetic shielding at extremely high frequencies, where (in contrast to the discussion for eddy currents) the displacement current cannot be neglected. In this regime, "good" conductors (which support plasmons) have a much richer behavior than "poor" conductors (which do not support plasmons).

Section VIII concludes with a discussion of the eddy current drag force (in the low-velocity, resistance-dominated limit) on a magnetic dipole falling down a conducting tube, such as can be strikingly demonstrated with the newly available neodymium–iron–boron magnets. Appendix A derives the uniqueness theorem for cases (such as those involving current loops) where it is more natural to employ the magnetic vector potential **A**. This case is nontrivial because, for a coil tipped at an arbitrary angle, the image potential $\mathbf{A}_I$ will have components in all three directions, whereas $\mathbf{A}_J$ from the actual induced currents will have only components in the plane. Finally, Appendix B contains a short survey of additional literature on eddy currents and MAGLEV.

II. MAXWELL'S RECEDING IMAGE CONSTRUCTION: SPONTANEOUS GENERATION OF A MONOPOLE

We illustrate Maxwell's receding image construction by considering the simplest case of all: the spontaneous generation, at $t=0$, of a monopole q^* at a height h above a thin conducting sheet. Unrealistic as this may appear, it can be simulated by a long, narrow, solenoid of radius $a \ll h$, whose near end is at the height h and whose far end is much further away than h. (We neglect the interesting issue of magnetic charge conservation, which would require a line of magnetic current leading to the materialized monopole from the other end of the solenoid.) The sheet is taken to be of conductivity σ and thickness d. In a geometrical sense, by "thin" it is meant that $d \ll h$. (There are other limitations, which will not be discussed until Sec. IV.) This example is considered because any magnetic disturbance can be treated by superimposing enough monopoles, which are created and destroyed at various times. In what follows, the expressions *induced currents, eddy currents,* and *induced eddy currents* are employed interchangeably.

According to the receding image construction, to an observer *below* the sheet, the magnetic field due to the induced currents arising when q^* is generated above the sheet will appear to arise from an image monopole $-q^*$ that, at $t=0^+$, sits precisely on top of the actual monopole, thereby cancelling the effect of the actual monopole. This first part of the construction satisfies the requirement that, at least initially, there be no change in magnetic flux within the conductor and, therefore, within the lower half-space. (As discussed in Sec. VII, within a suitable frequency range, there should be no change in magnetic flux within the interior of a closed conductor of any shape.) The second part of the receding image construction, which applies only for the thin sheet geometry, is that the image monopole appears to recede from the sheet to positive infinity, at the characteristic recession velocity

$$v_0 = 2/\mu_0 \sigma d, \tag{1}$$

where μ_0 is the permeability of free space. (This result will be derived in Sec. IV.) Thus, at finite time t, the image monopole $-q^*$ has the vertical position $h+v_0 t$. See Fig. 1. Because the image moves away from the surface, the eddy currents decay [see (7)], and the initially shielded magnetic field penetrates [see (8)].

To an observer *above* the sheet, the magnetic field due to the induced currents will appear to arise from an image monopole q^* that, at $t = 0^+$, sits at a distance h below the sheet. This, too, is to satisfy the requirement that, at least initially, there be no change in magnetic flux within the conductor. (This result holds only for a planar conductor.) At future times, this image monopole moves vertically to negative infinity at the characteristic velocity v_0. Thus, at finite time t, the image monopole q^* has the vertical position $-(h+v_0 t)$. See Fig. 1(b). Consideration of the force on the original monopole provides the essence of the theory of MAGLEV, which is discussed in more detail in Sec. VI.

In Maxwell's own words, "we conceive the state of things on the positive side of a certain closed or infinite surface (which is really caused by actions having their seat on that surface) to be due to an imaginary system on the negative side of the surface, which, if it existed, and if the action of the surface were abolished, would give rise to the actual state of things on the positive side of the surface."[4]

From the discontinuity in the field across the interface, one can compute the actual induced currents (the "actions having their seat on that surface") as a function of time. (The induced currents have already been given for a more realistic but somewhat more complex case, the creation of a magnetic dipole above a thin conducting sheet.[7]) Specifically, application of Ampere's law,

$$\nabla \times \mathbf{H} = \mathbf{J}, \tag{2}$$

to a circuit that just encloses the current sheet leads to a well-known relation between the field discontinuity across the sheet

$$\Delta \mathbf{B} = \mathbf{B}(0^+) - \mathbf{B}(0^-) \tag{3}$$

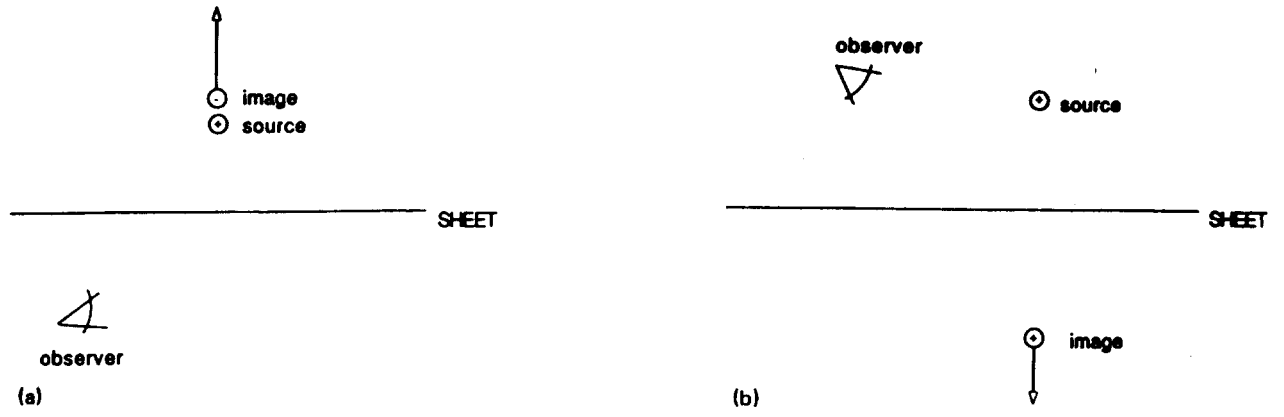

Fig. 1. (a) presents the system of monopole and image, as seen by an observer below the thin conducting sheet on the $z=0$ plane. The monopole q^* is spontaneously generated at $t=0$ a distance h above the sheet, and remains there at all times. The image $-q^*$ appears at the same place at $t=0^+$, and moves vertically upward at the velocity $v_0=2/(\mu_0\sigma d)$. (b) presents the system of monopole and image, as seen by an observer above the thin conducting sheet on the $z=0$ plane. The image q^* appears at the image position, h below the sheet, at $t=0^+$, and moves vertically downward at the velocity v_0.

$(0^{\pm}\equiv\pm d/2)$, and the surface current density $\mathbf{K}$:

$$\mathbf{K}=\int_{-d/2}^{d/2}\mathbf{J}\,dz=\hat{z}\times\Delta\mathbf{B}/\mu_0, \tag{4}$$

where $\mathbf{K}$ depends on the coordinates $\mathbf{x}$ and $\mathbf{y}$. In deriving (4), it was assumed that, outside the conductor,

$$\mathbf{B}=\mu_0\mathbf{H}. \tag{5}$$

In the present case, in units such that a monopole q^* at the origin produces a field $\mathbf{B}=(\mu_0 q^*/4\pi r^2)\hat{r}$, one has

$$\Delta\mathbf{B}=\frac{\mu_0 q^*\boldsymbol{\rho}}{2\pi[(h+v_0t)^2+\rho^2]^{3/2}}\ \text{(monopole creation)}, \tag{6}$$

where the origin is actually taken to be directly below the source monopole, and $\boldsymbol{\rho}=(x,y)$. Thus (4) yields

$$\mathbf{K}=\frac{q^*}{2\pi}\frac{\hat{z}\times\boldsymbol{\rho}}{[(h+v_0t)^2+\rho^2]^{3/2}}\ \text{(monopole creation)}. \tag{7}$$

This corresponds to a counterclockwise circulation of current as viewed from above. It is zero at the origin, has a peak for $\rho=\sqrt{1/2}(h+v_0t)$, and goes to zero as ρ^{-2} as $\rho\to\infty$. The induced currents have a circular pattern of flow, indeed satisfying the description of *eddy currents*. Note that the circulation of the electric field $\mathbf{E}$ around such a circuit is nonzero, an unmistakable indication that $\mathbf{E}$ is not of electrostatic origin.

The total field at the point $(0,0,-h)$ is given by

$$B_z^{\text{tot}}=-\frac{\mu_0 q^*}{4\pi}\left(\frac{1}{(2h)^2}-\frac{1}{(2h+v_0t)^2}\right); \tag{8}$$

and the field due to the induced currents, seen by the actual monopole:

$$B_z^{\text{ind}}=\frac{\mu_0 q^*}{4\pi}\left(\frac{1}{(2h+v_0t)^2}\right). \tag{9}$$

These are plotted in Fig. 2, with the fields given in units of $B_0=\mu_0 q^*/16\pi h^2$, and time in units of $t_0=v_0/2h$.

The reader, now familiar with the properties of Maxwell's receding image construction for this simplest of cases, should not have any difficulty with the next section, which sets out its properties in the more general case.

III. GENERAL PROPERTIES OF MAXWELL'S RECEDING IMAGE CONSTRUCTION

The theory has been phrased in terms of monopole sources. In the quasistatic approximation (instantaneous propagation of electromagnetic response) the magnetic field $\mathbf{B}$ thus can be obtained from a magnetic scalar potential Φ via

$$\mathbf{B}=-\nabla\Phi. \tag{10}$$

One contribution to the total potential arises from the arbitrary time-varying source potential Φ_s. It will be convenient to regard this as a superposition of suddenly appearing increments that are added at successive instants to produce the current value of the source potential. In addition to Φ_s, the total potential has a contribution Φ_J due to induced currents. Following Maxwell, we seek to replace Φ_J by the potential Φ_I due to a set of receding images. In the present section we obtain the properties of Φ_I, remarking on certain properties shared by Φ_I and Φ_J. This will

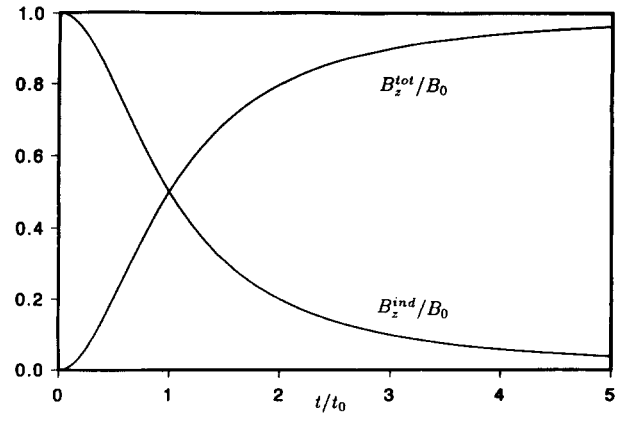

Fig. 2. Fields, as a function of time, when a monopole is generated at position $(0,0,h)$ and time $t=0$. The total field at $(0,0,-h)$, from (8), and the induced current contribution to the total field, at $(0,0,h)$, from (9), are plotted. The fields are given in units of $B_0=\mu_0 q^*/16\pi h^2$, and the time is given in units of $t_0=2h/v_0$.

enable us, after the boundary condition satisfied by Φ_J is obtained in Sec. IV, to employ the uniqueness theorem of electrostatics to show that Φ_J must be identical to Φ_I. In addition, we will derive the equations for Φ_I, (17) and (18), which later will be employed in Sec. V.

When the observer is in the lower half-space ($z < 0^-$), opposite to sources in the upper half-space ($z_s > 0^+$), both Φ_I and Φ_J satisfy Laplace's equation,

$$\nabla^2\Phi_{I,J}=0 \quad (z<0^-, z_s>0^+) \tag{11}$$

because the sources for both Φ_I and Φ_J are in the upper half-space; for Φ_I, the images are in the upper half-space, and for Φ_J the currents lie in the plane (i.e., the thin conducting sheet) above the lower half-space. Moreover, for localized sources, both Φ_I and Φ_J approach zero as $z\to -\infty$. Thus, according to the uniqueness theorem of electrostatics, if Φ_I and Φ_J satisfy the same boundary condition on $z = 0^-$, they must be equivalent.

The full image solution Φ_I will now be constructed, and from this, the partial differential equation satisfied by Φ_I. That will lead to the boundary condition satisfied by Φ_I on $z = 0^-$.

First by the receding image construction of the previous section, if from $t=u$ to $t = u^+ = u + \delta u$, there is a sudden change $\delta\Phi_s$ in the magnetic scalar potential Φ_s of the sources, the resulting contribution $\delta\Phi_I$ to Φ_I at some time $t>u$ is obtained by evaluating $-\delta\Phi_s$ with the sources receded a distance $v_0(t-u)$ upward. Equivalently, we can consider the sources as fixed and the effective observation point as receded downward:

$$\delta\Phi_I(x,y,z,t;u) = -\delta\Phi_s[x,y,z-v_0(t-u),u] \quad (z<0^-,t>u). \tag{12}$$

In (12), only the response to a delta-function source at $t=u$ was considered. By the principle of superposition and by the principle of causality one may add up the effect of contributions like that in (12), occurring in response to source changes at all times $u<t$, obtaining

$$\Phi_I(x,y,z,t) = \int_{-\infty}^{t} \delta\Phi_I(x,y,z,t;u) = -\int_{-\infty}^{t} du\frac{\partial_4}{\partial u}\Phi_s[x,y,z-v_0(t-u),u] \quad (z<0^-,z_s>0^+) \tag{13}$$

where the notation $\partial_4/\partial u$ means that in differentiating with respect to u, only the fourth argument of Φ_s is considered; u is held fixed in the third argument of Φ_s. Differentiation with respect to time of (13) then shows that Φ_I satisfies the differential equation

$$\frac{\partial}{\partial t}\Phi_I=-\frac{\partial}{\partial t}\Phi_s-v_0\frac{\partial}{\partial z}\Phi_I \quad (z<0^-,z_s>0^+), \tag{14}$$

where $\partial/\partial t$ acting on the upper limit in (13) contributes the first term on the right-hand side of (14), and $\partial/\partial t$ acting within the integral can be converted to $-v_0\partial/\partial z$, which then can be pulled outside the integral. In (14), the arguments of both Φ_I and Φ_s are (x,y,z,t). For later comparison, we rewrite (14) as

$$\frac{\partial}{\partial t}(\Phi_s+\Phi_I)=-v_0\frac{\partial}{\partial z}\Phi_I \quad (z<0^-,z_s>0^+). \tag{15}$$

Applied to $z = 0^-$, (15) may be thought of as providing a boundary condition on Φ_I.

Since (15) holds for all $z < 0^-$, its z derivative can be taken, thereby giving

$$\frac{\partial}{\partial t}(B_{sz}+B_{Iz})=-v_0\frac{\partial}{\partial z}B_{Iz} \quad (z<0^-,z_s>0^+). \tag{16}$$

In the next section, it will be shown that B_{Jz} satisfies an equation like (16), but only for $z = 0^-$.

To obtain the image solution for $z > 0^+$, it is useful to rewrite (13), the image solution for $z < 0^-$. Letting $\tau=t-u$, so $u=t-\tau$, (13) becomes

$$\Phi_I(x,y,z,t)=-\int_0^\infty d\tau\frac{d}{dt}\Phi_s(x,y,z-v_0\tau,t-\tau) \quad (z<0^-,z_s>0^+). \tag{17}$$

This $z < 0^-$ image solution may be transformed to the $z > 0^+$ image solution by replacing the image at $z_s > 0^+$ with one of opposite sign at $z_s' = -z_s$, and reflecting the image motion so that $z-v_0\tau$ for $z < 0^-$ goes to $z+v_0\tau$ for $z > 0^+$. With Φ_s' denoting a version of Φ_s with reflected sources, from (17) this construction leads to

$$\Phi_I(x,y,z,t)=\int_0^\infty d\tau\frac{d}{dt}\Phi_s'(x,y,z+v_0\tau,t-\tau) \quad (z>0^+,z_s'<0^-). \tag{18}$$

Equations (17) and (18) lead to a $\mathbf{B}_I$ for which B_{Iz} is even, and $\mathbf{B}_{I\perp}$ is odd, under reflection of z. This is also true of the actual solution due to the eddy currents, as discussed in Appendix A (Secs. 1 and 2).

To obtain the differential equation satisfied by Φ_I for $z>0^+$, use $u=t-\tau$ to put (18) in the form

$$\Phi_I(x,y,z,t)=\int_{-\infty}^{t} du\frac{\partial_4}{\partial u}\Phi_s'[x,y,z+v_0(t-u),u] \quad (z>0^+,z_s'<0^-). \tag{19}$$

by analogy to (13). Differentiation of (19) with respect to time yields

$$\frac{\partial}{\partial t}(-\Phi_s'+\Phi_I)=v_0\frac{\partial}{\partial z}\Phi_I \quad (z>0^-,z_s'<0^+), \tag{20}$$

the equation for $z > 0^+$ that is analogous to (15) for $z < 0^-$. This serves to emphasize that, for $z > 0^+$, not only do the images recede in the opposite direction, but they are obtained as the response to a source term with opposite sign and reflected source coordinates $z_s' = -z_s$.

Using (4) and (10), one can find the current density $\mathbf{K}$ directly in terms of the image potential, since only the discontinuity of the image potential contributes to $\mathbf{K}$. Specifically, taking Φ_I to be evaluated just above the sheet (so the image is on the opposite side from, and has the same sign as, the source), (4) becomes

$$\mathbf{K}=-\frac{2}{\mu_0}\hat{z}\times\nabla_\perp\Phi_I \quad (z\to 0^+). \tag{21}$$

Explicitly,

$$K_x=\frac{2}{\mu_0}\frac{\partial\Phi_I}{\partial y},\quad K_y=-\frac{2}{\mu_0}\frac{\partial\Phi_I}{\partial x}. \tag{22}$$

The quantity $-(2/\mu_0)\Phi_I$ is the same as Maxwell's current function.[3]

IV. DERIVATION OF AND CONSTRAINTS ON THE THEORY

A. Boundary condition on Φ_J

Consider an infinite planar conducting sheet of uniform thickness d and dc conductivity σ. Maxwell's equations including the presence of magnetic monopoles are

$$\nabla\cdot\mathbf{E}=\rho/\epsilon_0, \tag{23}$$

$$\nabla\cdot\mathbf{B}=\mu_0\rho^*, \tag{24}$$

$$\nabla\times\mathbf{E}=-\mu_0\left(\mathbf{J}^*+\frac{1}{\mu_0}\frac{\partial\mathbf{B}}{\partial t}\right), \tag{25}$$

$$\nabla\times\mathbf{B}=\mu_0\left(\mathbf{J}+\epsilon_0\frac{\partial\mathbf{E}}{\partial t}\right), \tag{26}$$

which imply the conservation laws for charge and monopole density:

$$\frac{\partial\rho}{\partial t}+\nabla\cdot\mathbf{J}=0, \tag{27}$$

$$\frac{\partial\rho^*}{\partial t}+\nabla\cdot\mathbf{J}^*=0, \tag{28}$$

where $\mathbf{J}^*$ is the monopole current density.

To obtain the quasistatic approximation, we assume that Maxwell's own displacement current $\epsilon_0\,\partial\mathbf{E}/\partial t$ in (26) may be neglected, both inside and outside the conductor. As a consequence, the divergence of (26) implies that $\nabla\cdot\mathbf{J}=0$, which by (27) leads to a charge density that does not vary with respect to time. Since we are concerned with time-varying properties, we neglect any static terms, and thus consider that $\rho=0$.

We also neglect the effect of surface charge, which is localized to within a thickness a on the order of an inverse Fermi wavelength in the case of a metallic conductor, and to within a Debye–Huckel screening length in the case of a poor conductor. (In this planar geometry the surface charges on opposing surfaces are equal and opposite, producing an electrostatic field that is strictly internal.) Note that, because of the large effective resistance to flow through a channel of narrow thickness a, the surface currents are small. (In this planar geometry the surface currents on opposing surfaces are equal and opposite, producing a magnetic field that is strictly internal, and transverse to the direction of the surface currents.) As with the problem of a charge moving parallel to a conductor,[8] the surface charge is brought to the surface by interior currents normal to the sheet. In Sec. IV C we argue that, in the quasistatic approximation, the magnetic field produced by these interior currents may also be neglected.

Since in practice we will be interested in the boundary conditions at the surface of the conductor, and the monopole sources are zero there, we may neglect ρ^* and $\mathbf{J}^*$, leading to a set of equations whose only explicit source lies within the conductor:

$$\nabla\cdot\mathbf{E}=0, \tag{29}$$

$$\nabla\cdot\mathbf{B}=0, \tag{30}$$

$$\nabla\times\mathbf{E}=-\frac{\partial\mathbf{B}}{\partial t}, \tag{31}$$

$$\nabla\times\mathbf{B}=\mu_0\mathbf{J}. \tag{32}$$

To these we add

$$\mathbf{J}=\sigma\mathbf{E} \tag{33}$$

within the conductor. From the curl of (32), and with use of (30), (31), and (33), it is straightforward to derive the field diffusion equation

$$\nabla^2\mathbf{B}=\mu_0\sigma\frac{\partial\mathbf{B}}{\partial t}. \tag{34}$$

Because of the boundary condition that the normal component of $\mathbf{B}$ (i.e., $\mathbf{B}\cdot\hat{n}$) is continuous across any interface, a well-known result that follows from (30), and because currents in the sheet itself do not cause $\mathbf{B}\cdot\hat{n}$ to change suddenly as one crosses through the sheet, we focus on the normal component of (34). This enables one to learn about the field just outside of the conductor, on the basis of what is happening just inside the conductor. At this point, it becomes relevant to consider a number of consequences to the assumption that the sheet is thin.

We take the source to be of some characteristic strength q^*, at a characteristic distance h from the sheet. The characteristic field strength is then $B_0=\mu_0 q^*/h^2$, and characteristic field gradients outside the conductor are on the order of B_0/h, both for B_s and B_J. Moreover, the characteristic field gradients of B_s inside the conductor are also of order B_0/h.

However, although B_{Jz} has the same value on both sides of the conductor, as follows from the Biot–Savart law for the field on the same plane as the current sources, its derivative $\partial_z B_{Jz}\sim B_0/h$ changes sign on passing through the conductor. Hence, $\partial_z^2 B_{Jz}\sim\partial_z^2 B_z\sim B_0/hd$ within the conductor. On the other hand, $\partial_\perp^2 B_z\sim B_0/h^2$. As a consequence, the dominant part in the Laplacian of B_z arises from the normal derivatives, so that the transverse derivatives will be neglected. This permits the left-hand side of (34) to be integrated exactly in the direction of the normal. Note that B_z changes by only $(\partial_z B_{Jz})d\sim B_0(d/h)\ll B_0$ on crossing the sheet, so that B_z is nearly uniform across the cross section.

Taking the normal $\hat{n}$ to point toward the side of the source ($\hat{n}=\hat{z}$ in the example of Sec. II), integration of (34) across the sheet yields, with $\nabla^2\approx\partial^2/\partial z^2$,

$$-\Delta\left(\frac{\partial B_z}{\partial z}\right)=-\left(\frac{\partial B_z(0^-)}{\partial z}-\frac{\partial B_z(0^+)}{\partial z}\right)$$
$$=(\mu_0\sigma d)\frac{\partial B_z}{\partial t}\quad(z<0^-,z_s>0^+). \tag{35}$$

The left-hand side of (36) may be rewritten, in a sequence of steps, via

$$\Delta\left(\frac{\partial B_z}{\partial z}\right)=-\Delta(\nabla_\perp\cdot\mathbf{B}_\perp)=-\Delta(\nabla_\perp\cdot\mathbf{B}_{J\perp})$$

$$= -2\nabla_\perp \cdot \mathbf{B}_{J\perp}|_{z=0^-} = 2\left.\frac{\partial B_{Jz}}{\partial z}\right|_{z=0^-}. \quad (36)$$

The first equality arises from (30); the second occurs because the discontinuity in the transverse component of the field, on crossing the sheet, is due only to the currents on the sheet; the third occurs because the transverse component of the sheet changes sign on crossing the sheet; the fourth arises, again, from (30). With (36) and (1), one may rewrite (35) for the field on the side opposite the source as

$$\frac{\partial}{\partial t}(B_{Jz}+B_{sz}) = -v_0\frac{\partial B_{Jz}}{\partial z} \quad (z=0^-, z_s>0^+), \quad (37)$$

where both the source and current contributions to B_z have been written explicitly. This is the desired boundary condition on $B_{Jz} = -\partial\Phi_J/\partial z$.

It will now be shown that the uniqueness theorem of electrostatics guarantees that the problem is completely defined, with a unique solution, and that $\Phi_I = \Phi_J$.

B. Uniqueness theorem

Given that B_{sz} is known at any instant, as is $\partial B_{Jz}/\partial z$, one can compute from (37) the change in B_{Jz} after a time-interval δt. With this knowledge, one can in principle solve Laplace's equation for Φ_J (if necessary, by computer) subject to its new normal derivative $\partial\Phi_J/\partial z = -B_{Jz}$ on the sheet, and the condition that Φ_J vanish at infinity. The uniqueness theorem of electrostatics applies to this case, since: (1) Laplace's equation is satisfied in the observation region $z < 0^-$; (2) $\Phi_J \to 0$ as $z \to -\infty$; and (3) the normal derivative of Φ_J is specified on $z = 0^-$. Hence, both Φ_J and its field $\mathbf{B}_J$ are uniquely determined for all $z<0$. The resulting $\partial\Phi_J/\partial z$ can be used in (37) for the next instant to repeat the argument, and thus the solution can be propagated in time.

From (16), it was shown that B_{Iz} also satisfies (37). Because of the uniqueness theorem of electrostatics, this guarantees that B_{Iz} and B_{Jz}, and hence Φ_I and Φ_J, are equivalent in the lower half-plane. Similar considerations apply to Φ_I and Φ_J in the upper half-plane. The equivalence of the image solution Φ_I to the eddy current solution Φ_J has thus been established.

In Sec. V, examples of the use of the image solution equations, (17) and (18), are given. Before that, however, we consider a number of conditions defining the range of validity of the theory.

C. Constraints on the theory

Although it was not relevant to the monopole example of Sec. II, in typical circumstances there will also be a characteristic time τ_1, and it is subject to a number of constraints. To better appreciate these constraints, it will be useful to distinguish between "good" and "poor" conductors.

We shall employ the Drude ac conductivity for a material with only one type of charge carrier:[9]

$$\sigma(\omega) = \sigma_0/(1-i\omega\tau). \quad (38)$$

In this section only, we employ σ_0 (rather than σ) for the dc conductivity, which is given by

$$\sigma_0 = \frac{ne^2\tau}{m} = \frac{\omega_p^2\tau}{\mu_0 c^2}, \quad \omega_p^2 \equiv \frac{ne^2}{m\epsilon_0} \quad (\mu_0\epsilon_0 c^2 = 1), \quad (39)$$

where the charge carriers have number density n, charge e, mass m, and ω_p is the plasma frequency. Note that Maxwell lived in a time before the discovery of the electron, and had no basis for anything but a dc conductivity.

We define a "good" conductor as one that will support plasma oscillations, and a "poor" conductor as one that will not. This is determined by looking for underdamped solutions to (23), (27), (33), and (38). Such solutions occur for $\omega_p\tau > 1/2$.[9] Thus we define good conductors and poor conductors using the criteria

$$\omega_p\tau > 1/2 \text{ (good conductor)}, \quad (40)$$

$$\omega_p\tau < 1/2 \text{ (poor conductor)}. \quad (41)$$

We now turn to the constraints on the theory.

(1) For the dc conductivity to be employed, the inequality

$$\tau_1 \gg \tau \text{ (good conductor)} \quad (42)$$

must be satisfied, where τ is the electronic relaxation time. This relationship is satisfied for all conductors, but for poor conductors this is less restrictive than the following condition.

(2) For the quasistatic approximation to be valid within the conductor, the displacement current must be negligible. This implies

$$\tau_1 \gg \epsilon_0/\sigma_0 = (\omega_p^2\tau)^{-1} \text{ (poor conductor)}. \quad (43)$$

This relationship is satisfied by all conductors, but for good conductors it is less restrictive than (42). One may verify that (42) implies (43) for a good conductor, and that (43) implies (42) for a poor conductor, by use of (40) and (41), as appropriate.

Thus, for a poor conductor, as the frequency increases, one must first correct the theory by including the displacement current, and then by letting the response become dominated by the inertia of the charge carriers. For a good conductor, on the other hand, as the frequency increases, one must first correct the theory by letting the response become dominated by the inertia of the charge carriers, and then by including the displacement current.

(3) For the quasistatic approximation to be valid outside the conductor, the displacement current must be negligible. Equivalently, the signal from the source must arrive much more quickly than changes occur in the source, or

$$h/c \ll \tau_1. \quad (44)$$

(4) τ_1 must be long enough for diffusion to occur across the thickness d of the conductor, so that time variations due to the changes in the source can be "instantaneously" followed by the diffusion process. From (34), that means

$$\tau_1 \gg \mu_0\sigma_0 d^2 \sim d/v_0. \quad (45)$$

This is equivalent to the statement that the electromagnetic skin depth

$$\delta(\omega) = \sqrt{2/(\mu_0\sigma_0\omega)} \quad (46)$$

satisfies $\delta \gg d$.

The Maxwell recession velocity v_0 need not be less than the velocity of light, provided the other conditions are satisfied. The images do not actually exist, and thus no real object is relativistic if $v_0 > c$. As an example, let us take for sea water $\sigma_0 \approx 4$ (ohm $-$ m)$^{-1}$. For 60 Hz ac power, the skin depth is about 32 m, and thus a 1-mm thickness of sea water satisfies the conditions for the receding image construction to apply, with $v_0 \approx 4\times 10^8$ m/s $> c$.

Note that the diffusion equation and our earlier discussion of the spatial variation of B_z implies that

$$\partial_t B_z \sim B_0/(h\, d\sigma_0\mu_0) \sim B_0 v_0/h \tag{47}$$

inside the conductor. [This can be seen explicitly in the monopole example of Sec. II, where (8) has this property.] As a consequence, any rapid change in the sources will be shielded out for a characteristic time $t_0 \sim h/v_0$. For a rapid transient in a power line 10 m above a 1 mm thickness of sea water, t_0 is about 25 nanosecond. For a 1-mm thickness of copper, however, where $\sigma_0 \approx 6\times 10^7$ (ohm$-m$)$^{-1}$, t_0 is about one-third of a second.

We close this section with an estimate of the magnitude of the field B' induced by the interior currents, alluded to in Sec. IV A. First, by Ampere's law, the characteristic induced electric field $E' \sim \omega h B_s$. Second, by the boundary condition on the electric field, the surface charge density $\sigma' \sim \epsilon_0 E' \sim \epsilon_0 \omega h B_s$. Third, by the charge continuity equation applied at the surface, the interior current density $J_z \sim \partial\sigma'/\partial t \sim \omega^2 h \epsilon_0 B_s$. Fourth, from the Biot–Savart law, for a sheet of thickness d,

$$B' \sim \mu_0(\omega^2 h\epsilon_0) d \int \frac{B_s}{R^2}\, dS'$$

$$\sim (\omega^2 h d/c^2) B_s \sim (\omega h/c)^2 (d/h) B_s,$$

where we take $R \sim h$ and $B_s \sim \mu_0 J_z d$. [The surface current density $K' \sim \omega a \sigma' \sim \omega^2 a h \epsilon_0 B_s$, and it produces a field $B'_K \sim \mu_0 K' \sim (\omega^2 a h/c^2) B_s \sim (a/d) B'$ which is much less than B'.] Thus, with $\omega^{-1} \to \tau_1$, if (44) holds, then the field B' due to the interior currents can be neglected.

V. IMAGE POTENTIAL SOLUTIONS— OSCILLATING MONOPOLE AND DIPOLE

As an example of the use of the receding image method, let us consider a monopole of oscillating strength $q^* \cos \omega t$ located at $(x_s,y_s,z_s) = (0,0,h)$, and the image potential it produces at $(0,0,z)$, for $z<0$. (Such a monopole can be simulated if the long solenoid of Sec. II is subject to an ac voltage.) In that case

$$\Phi_s(0,0,z,t) = \Phi_0 \cos \omega t,\ \Phi_0 = \frac{\mu_0 q^*}{4\pi(h-z)}\ (z<0), \tag{48}$$

and application of (17) for the side opposite the source then leads to

$$\Phi_I(0,0,z,t)$$

$$= -\frac{\mu_0 q^* \omega}{4\pi v_0} \cos \omega t [\sin p\, \mathrm{ci}(p) - \cos p\, \mathrm{si}(p)]$$

$$-\frac{\mu_0 q^* \omega}{4\pi v_0} \sin \omega t [\sin p\, \mathrm{si}(p) + \cos p\, \mathrm{ci}(p)]$$

$$[p = \omega(h-z)/v_0], \tag{49}$$

where[10]

$$\mathrm{ci}(p) \equiv -\int_p^\infty \frac{\cos x}{x}\, dx,\ \mathrm{si}(p) \equiv -\int_p^\infty \frac{\sin x}{x}\, dx. \tag{50}$$

This shows that, at low ω, the response of the induced currents is proportional to ω, disappearing in the static limit, as one would expect physically. One can also evaluate this in the high-frequency limit; however, another development due to Maxwell is particularly appropriate to high frequencies.

In (17), the derivative with respect to t may be replaced by a partial derivative with respect to τ in the fourth argument. Then, since for any function $f(x,y,z-v_0\tau,t-\tau)$, as appears in (17),

$$\frac{d}{dt} f = -\frac{\partial_4}{\partial\tau} f = -\frac{d}{d\tau} f + \frac{\partial_3}{\partial\tau} f = -\frac{d}{d\tau} f - v_0 \frac{d}{dz} f, \tag{51}$$

one can rewrite (17) as

$$\Phi_I(x,y,z,t) + \Phi_s(x,y,z,t)$$

$$= v_0 \frac{d}{dz} \int_0^\infty d\tau\, \Phi_s(x,y,z-v_0\tau,t-\tau)$$

$$(z<0^-, z_s>0^+). \tag{52}$$

In obtaining this result, the contribution from the $\tau \to \infty$ upper limit of the integral in (17) is taken to be zero, since it corresponds to sources that have receded infinitely far away. Equation (52) is particularly appropriate when the source undergoes very rapid time variations, for then one can see that the net amount of field penetration is down by a factor $v_0/(\omega h)$, where ω and h are the characteristic frequency and position of the source.

Application of (52) to the present case then leads to

$$\Phi_I(0,0,z,t) + \Phi_s(0,0,z,t)$$

$$= \frac{\mu_0 q^*}{4\pi} \int_0^\infty ds \frac{\cos \omega(t - s/v_0)}{(h-z+s)^2}, \tag{53}$$

which, on repeated integration by parts, gives

$$\Phi_I(0,0,z,t) + \Phi_s(0,0,z,t)$$

$$= \Phi_0 \left(\frac{\sin \omega t}{p} + \frac{2\cos \omega t}{p^2} + O(p^{-3}) \right)$$

$$[p = \omega(h-z)/v_0]. \tag{54}$$

This shows that the leading term of the net response in the high-frequency limit is out-of-phase and down by a factor of $p^{-1} \sim \omega^{-1}$ from the source term. Moreover, the next in-phase response is down by a factor of ω^{-2}.

Application of (18) for the same side as the source leads to the result, for $z>0$,

$$\Phi_I(0,0,z,t) = \frac{\mu_0 q^* \omega}{4\pi v_0} \cos \omega t [\sin p\, \mathrm{ci}(p) - \cos p\, \mathrm{si}(p)]$$

$$+ \frac{\mu_0 q^* \omega}{4\pi v_0} \sin \omega t [\sin p\, \mathrm{si}(p) + \cos p\, \mathrm{ci}(p)]$$

$$\times [p = \omega(h+z)/v_0], \tag{55}$$

which is very similar to the result below the sheet. The force on the monopole itself is then given by

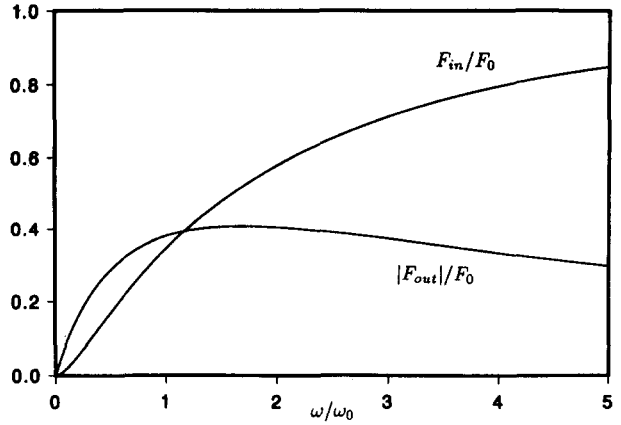

Fig. 3. Forces, as a function of frequency, on a monopole of oscillating strength, due to eddy currents, computed from (56). Both the in-phase component (labeled "in") and the out-of-phase component (labeled "out") are given. The forces are given in units of the force $F_0=\mu_0 q^{*2}/16\pi h^2$ due to an image below the monopole, and the frequency is given in units of $\omega_0=v_0/2h$.

$$F_{Iz}=q^*\cos\omega t\left(-\frac{\partial\Phi_I}{\partial z}\bigg|_{z=h}\right)$$
$$=-\frac{\mu_0 q^{*2}}{16\pi h^2}\cos^2\omega t\cdot p^2[\cos p\,\mathrm{ci}(p)+\sin p\,\mathrm{si}(p)]$$
$$-\frac{\mu_0 q^{*2}}{16\pi h^2}\sin\omega t\cos\omega t\cdot p^2\left[\frac{1}{p}+\cos p\,\mathrm{si}(p)\right.$$
$$\left.-\sin p\,\mathrm{ci}(p)\right]\quad(p=2\omega h/v_0). \tag{56}$$

Figure 3 gives the frequency dependence of the amplitudes of the in-phase part F_{in} (coefficient of $\cos^2\omega t$), and of the out-of-phase part F_{out} (coefficient of $\sin\omega t\cos\omega t$), of this force. The forces are given in units of $F_0=\mu_0 q^{*2}/16\pi h^2$, and the frequency is given in units of $\omega_0=v_0/2h$. (Note that F_{out} is negative, so that its magnitude is plotted.) From the behavior of $\mathrm{ci}(p)$ and $\mathrm{si}(p)$ for large p, it is straightforward to show that at high frequencies (56) approaches the field of a completely flux-expelling image. In Sec. VII it is shown that to obtain the drag at low frequencies one need consider only the current induced by the applied field; we have verified that the low-frequency limit of (56) is in agreement with such a calculation.

As with the monopole creation example, the present example does not conserve magnetic charge. Magnetic charge would be conserved were a magnetic current $I^*=-\omega q_0^*\sin\omega t$ to move up the z axis from the monopole. That would produce a solenoidal electric field in the sheet, with

$$\mathbf{E}=\frac{\mu_0\omega q_0^*\sin\omega t}{4\pi}\left(1-\frac{h}{\sqrt{\rho^2+h^2}}\right)\hat{\phi}, \tag{57}$$

with a corresponding magnetic field

$$\mathbf{B}'=\frac{\mu_0 q_0^*}{4\pi}\cdot\frac{\omega h}{v_0}\cdot\frac{\sin\omega t}{2h^2}\cdot\hat{k}. \tag{58}$$

The force this produces on the monopole,

$$F_z'=\frac{\mu_0 q^{*2}}{16\pi h^2}\cdot p\cdot\sin\omega t\cos\omega t\quad(p=2\omega h/v_0), \tag{59}$$

cancels out the leading $\sin\omega t\cos\omega t$ term in (56).

From the oscillating monopole case one can obtain the more realistic case of an oscillating dipole. Specifically, consider a dipole whose moment points vertically upward from the plane, corresponding to a small current loop whose plane is parallel to the conducting sheet. In that case we take, instead of (48),

$$\Phi_s(0,0,z,t)=\Phi_0\cos\omega t,\quad \Phi_0=-\frac{\mu_0 m}{4\pi(h-z)^2}\quad(z<0). \tag{60}$$

Employing this in (18) yields

$$\Phi_I(0,0,z,t)$$
$$=\frac{\mu_0 m\omega^2}{4\pi v_0^2}\int_0^\infty\frac{dx\sin(\omega t-x)}{(p+x)^2}\quad[p=\omega(h+z)/v_0] \tag{61}$$

for $z>0$. We employ this to find the force on the dipole due to the eddy currents, from

$$F_{Iz}=-m\cos\omega t\,\frac{\partial^2\Phi_I}{\partial z^2}\bigg|_{z=h}. \tag{62}$$

In the high-frequency limit the leading terms are

$$F_{Iz}=\frac{3\mu_0 m^2}{32\pi h^4}\cos^2\omega t-\frac{3\mu_0 m^2 v_0^2}{16\pi h^5\omega}\sin\omega t\cos\omega t, \tag{63}$$

whereas in the low-frequency limit the leading terms are

$$F_{Iz}=-\frac{\mu_0 m^2\omega}{16\pi v_0 h^3\omega}\sin\omega t\cos\omega t+\frac{\mu_0 m^2\omega^2}{16\pi v_0^2 h^4}\cos^2\omega t. \tag{64}$$

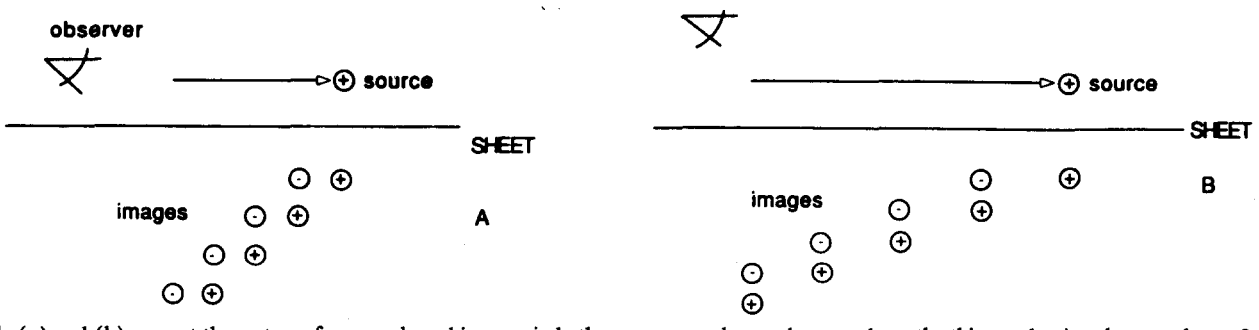

Fig. 4. (a) and (b) present the system of monopole and images, in both cases as seen by an observer above the thin conducting sheet on the $z=0$ plane. The monopole q^* moves at a constant velocity $\mathbf{v}$ parallel to the sheet; (a) corresponds to a low velocity, and (b) to a high velocity. The train of positive and negative images appear at infinitesimal intervals in response to the motion of the monopole, each movement of the monopole being equivalent to the appearance of a positive and negative monopole at the new and old image positions. The images, once generated, move vertically downward at the velocity v_0.

In both cases, the leading terms (from the flux-expelling image, at high frequencies, and from the currents induced by the applied field only, at low frequencies) agree with direct calculations of the force.

In the next section we consider some additional applications of Maxwell's receding image construction, returning to the original statement of the construction to derive some results that are basic to an intuitive understanding of MAGLEV.

VI. MAXWELL, MAGLEV, AND ARAGO'S DISK

As stated in the Introduction, the basic principles for magnetic levitation by eddy were laid out by Maxwell in 1872.[4] There, as his second application of the receding image construction—the first application was to the force on a monopole moving toward a thin conducting sheet—he calculated the lift and drag force on a monopole moving at a constant velocity parallel to a thin conducting sheet. Because of its importance, it will be reproduced here. Note that the calculation was included in Sec. 665 of Maxwell's Treatise,[3] where he gives a drag force differing from that in the original paper. The calculation was later done by Reitz,[11] who found a result in agreement with that in the Treatise. Reitz also considered a number of other cases. Despite the fact that (19) can be applied directly to this case, we will follow Maxwell's original, visually intuitive approach, because it suggests what occurs even for nonuniform motion.

A. Monopole moving parallel to a thin conducting sheet

Consider a monopole moving at a velocity v parallel to a thin conducting sheet, at a height h. Following Maxwell,[3] if in $z>0^+$ a monopole moves with velocity v along the x direction, creating pairs of equal and opposite images with each increment in its motion (*equal* at the new image position, and *opposite* at the old image position, to effect a cancellation), then two trains of images are produced, one positive and one negative, each with slope v_0/v. In the limit as $v \gg v_0$, all of the image monopoles will nearly cancel (the negative image created at t will nearly cancel the positive image created at $t-\delta t$, because the image hardly moves in the time interval δt), *except* the latest positive image. See Fig. 4, where sets of images has been drawn corresponding to $v \sim v_0$ and $v \gg v_0$. Hence, for $v \gg v_0$ the sheet behaves like a superconductor, and repels the monopole with an image monopole.[7]

Returning to the general case, explicitly summing over the images induced at different times $n\tau=t'$, and passing to the limit where $\Delta n\tau=\tau=dt'$, one finds that

$$\begin{aligned}\Phi_I(x+vt,0,z,t)&=\frac{\mu_0 q^*}{4\pi}\sum_n\left[\frac{1}{\sqrt{(z+h+nv_0\tau)^2+(x+nv\tau)^2}}-\frac{1}{\sqrt{(z+h+nv_0\tau)^2+(x+(n+1)v\tau)^2}}\right]\\&=\frac{\mu_0 q^*}{4\pi}\int_0^\infty\frac{(x+vt')v\,dt'}{[(z+h+v_0t')^2+(x+vt')^2]^{3/2}}\\&=\frac{\mu_0 q^*}{4\pi}\frac{v}{[(z+h)^2v^2-2vv_0(z+h)x+v_0^2x^2]}\left[\frac{v_0^2x-vv_0(z+h)}{\sqrt{v_0^2+v^2}}-\frac{v_0(z+h)x-v(z+h)^2}{\sqrt{(z+h)^2+x^2}}\right],\end{aligned}\tag{65}$$

$$\Phi_I(vt,0,z,t)=\frac{\mu_0 q^*}{4\pi(z+h)}\left(1-\frac{v_0}{\sqrt{v^2+v_0^2}}\right),\tag{66}$$

where the latter form, evaluated at a point with the same x coordinate as the moving monopole, is useful in obtaining the lift.

Note that, with t' replaced by τ, (65) could have been obtained directly from (19). However, the present derivation and the associated physical picture immediately gives the $v \gg v_0$ limit, something that does not appear in (65) until after the integral has been done. Moreover, at high velocities, but with a more complex type of motion, the construction clearly shows the dominance of the latest image, so that physics may be extracted even when the corresponding integral from (19) is not tractable.

Evaluating the appropriate gradients in (65) and (66), and then setting $x=0$ and $z=h$ gives magnetic field components that lead to

$$F_L=-q^*\frac{\partial\Phi_I}{\partial z}=\frac{\mu_0 q^{*2}}{16\pi h^2}\left(1-\frac{v_0}{\sqrt{v^2+v_0^2}}\right),\tag{67}$$

$$F_D=-q^*\frac{\partial\Phi_I}{\partial x}=\frac{\mu_0 q^{*2}}{16\pi h^2}\frac{v_0}{v}\left(1-\frac{v_0}{\sqrt{v^2+v_0^2}}\right).\tag{68}$$

These are plotted in Fig. 5, where the forces are given in units of the force $F_0=\mu_0 q^{*2}/16\pi h^2$ due to the latest positive image, and the velocity is given in units of v_0. Comparison to Fig. 3 shows that (v_0,F_L,F_D) are analogous to $(\omega h,F_{\text{in}},-F_{\text{out}})$.

To our knowledge, the earliest reference to eddy current MAGLEV is a 1912 report in *The Engineer* on a working model built by Bachelet.[12] In the 1960s and 1970s there was a revival of interest in eddy current MAGLEV, as can be seen in the work of Powell and Danby,[13] Guderjahn *et al.*,[14] Reitz,[11] Reitz and Davis,[15] Coffey *et al.*,[16] and Richards and Tinkham.[17] Shortly before such interest in MAGLEV, Hannakam considered the eddy currents induced in a thin conducting sheet, using a Fourier space formalism to solve for the eddy current response to two parallel current-carrying wires moving relative to the conductor.[18]

B. General relation between lift and drag

Both Hannakam and Reitz observed that, for all the cases they considered, which involved sources of magnetic field moving with velocity v parallel to a thin conducting

sheet (this includes the case just considered), there is a simple relationship between the lift force F_L and the drag force F_D:

$$F_D/F_L=v_0/v, \tag{69}$$

where v_0 is the characteristic recession velocity (1). [Clearly F_D and F_L of (67) and (68) satisfy this relationship.] Davis has established this as a general result using the Poynting vector;[19] it will now be established using the properties of Maxwell's receding image construction.

Consider a source of magnetic field (e.g., a magnet, of arbitrary size and shape) moving with velocity v parallel to a thin conducting sheet. Because of the drag and lift forces, unless the magnet is acted on by opposing forces, it will slow down and move away from the sheet. Let us therefore apply forces that are equal and opposite to the drag and lift forces, so that no net force acts on the magnet, and it thus continues to move at the constant velocity v parallel to the sheet. The vertical component of the applied force provides no power, since there is no vertical motion. However, the horizontal component of the applied force, which is equal and opposite to the drag force, provides a power $F_D v$. This power must go into the dissipation of the eddy currents, whose magnetic field can be reproduced by a receding train of image magnets, as in Fig. 4. The dissipation rate into the eddy currents may also be calculated by considering the energy that must be put into the receding train of image magnets. This train of image magnets moves only in the vertical direction, with a velocity v_0. It feels a net vertical force that, by Newton's second law, must be equal and opposite to the lift force. Hence, the power going into the receding train of images is given by $F_L v_0$. Equating the power going into the eddy currents with the power going into pushing the train of images away from the sheet then yields (69).

The reader who is skeptical about the literal way in which images are employed in this argument should note that all energy calculations can be done by employing the Poynting vector, and by the uniqueness theorem both the images and the actual eddy currents give the same Poynting vector. If the Poynting vector calculation of the rate at which energy is being dissipated did not equal the rate of work on the images, then the train of images would not be in the steady state, in contradiction to the assumption of uniform motion. Note that the Poynting theorem still holds when, as in the case of the present theory, the displacement current is neglected, the only difference from the usual case being that the energy stored in the electric field is not included.

One consequence of (69) is that, at low v, where in general one expects that $F_D \sim v$, one concludes that $F_L \sim v^2$. A second consequence of (69) is that, at high v, where the lift force is the same as the image force, and thus is independent of v, the drag force goes as v^{-1}. Equivalently, at high v, the power dissipation is a constant, independent of v, given by the product of the image force and the recession velocity v_0. Finally, it should be noted that the drag force, going to zero at both low and high velocity, has a maximum at an intermediate value. Thus, in the acceleration process, the MAGLEV train's motor must get it over this "hump" before the train can accelerate to its full speed, which will be limited primarily by aerodynamic drag. These velocity dependences are seen explicitly for the case of a monopole in Fig. 5.

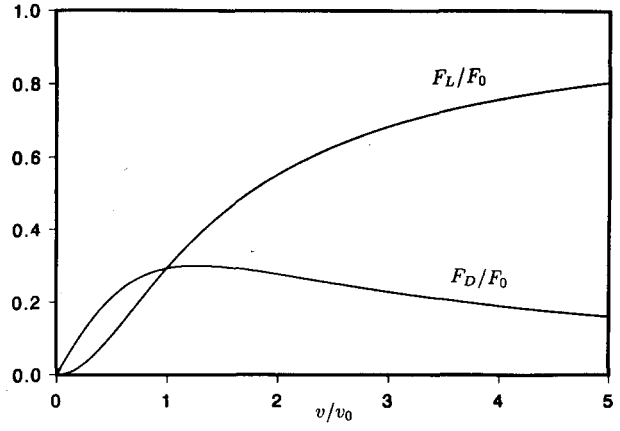

Fig. 5. The lift and drag forces, as a function of velocity, on a monopole moving at a constant velocity v at a height h above a thin conducting sheet, computed from (67) and (68). The forces are given in units of the force due to the latest positive image $F_0=\mu_0 q^{*2}/16\pi h^2$, and the velocity is given in units of v_0.

C. Arago's disk

In 1825, prompted by the observation that his compass needle came to rest more quickly when it was inside its metallic case than when it was outside, Arago suspended a magnetic needle above a rotating metallic disk, and found that the needle tended to come into rotation with the disk.[20] This phenomenon was so much on Faraday's mind that, early in the paper in which he announced what has come to be known as Faraday's law, Faraday wrote "I lately...obtained a key which appeared to me to open out a full explanation of Arago's magnetic phenomenon..."[21]

Faraday's interest became Maxwell's: in his Treatise, Maxwell considers a disk of radius a spinning at the rate ω, in an external field, developing the general theory, but not working out its details. In one of the editorial footnotes to the third edition of Maxwell's Treatise, J. J. Thomson gives quantitative expressions for the drag force, the lift force, and the force toward the center for a monopole at a height h and radius r, for small ω and $r \ll a$. In fact, in this low velocity limit, the lift and drag can be obtained from the results for linear motion. Moreover, if one considers the velocity $v=\omega r$, and differentiates with respect to r, one can also obtain the radial force. Specifically, with (66) for Φ_I, at low velocities one has

$$U=q^*\Phi_I(vt,0,z,t)=\frac{\mu_0}{4\pi}\frac{q^{*2}r^2\omega^2}{2(z+h)v_0^2}, \tag{70}$$

$$F_L=-\left.\frac{\partial U}{\partial z}\right|_{z=h}=\frac{\mu_0}{4\pi}\frac{q^{*2}r^2\omega^2}{8h^2v_0^2}, \tag{71}$$

$$F_{\rm rad}=-\frac{1}{2}\left.\frac{\partial U}{\partial r}\right|_{z=h}=-\frac{\mu_0}{4\pi}\frac{q^{*2}r\omega^2}{4hv_0^2}, \tag{72}$$

$$F_D=F_L\frac{v_0}{r\omega}=\frac{\mu_0}{4\pi}\frac{q^{*2}r\omega}{8h^2v_0}. \tag{73}$$

[The factor of 1/2 in (72) is due to the fact that the potential is self-induced; if z had been set to h before the differentiation in (71), a similar factor of 1/2 would have

appeared.] In the limit of large rotation rates, one would not be able to utilize the linear motion results to obtain the rotational motion results.

It is worth remarking that, as expected, the radial force does not change direction when $\omega \rightarrow -\omega$. Indeed, for $\omega a/v_0 \ll 1$ this force is proportional to ω^2. The direction of this force is in agreement with the discussion of the next section, where we argue that the most general form of Lenz's law says that induced currents will lead to a magnetic force in the direction that most effectively decreases the rate of Joule heating. In the present case, in order to move the monopole away from a region of changing flux, the force is directed toward the center (at the center, the field does not appear to change at all). However, for the monopole near the edge of the disk (where one cannot perform the calculation easily) this force will be directed away from the center (at infinity the field does not change at all). Maxwell obtains this same qualitative result by consideration of induced images. Of course, the drag and lift forces also satisfy Lenz's law: the drag force decreases the relative motion and thus decreases the amount of the induced currents; and the lift force moves the monopole away from the magnetic field of the induced currents, and thus also decreases the amount of the induced currents.

Maxwell comments, in Sec. 669 of Ref. 3, that "the equations necessary for determining the induction of the currents on themselves are given [by E. Jochmann in Pogg. Ann. CXXII, p. 214 (1864)], but this part of the action [the induction of the currents on themselves—that is, self-inductance effects] is omitted in the subsequent calculation of results." (The bracketed remarks have been added for clarity.) In other words, Jochmann had performed a calculation of the induced currents in the limit where the eddy currents themselves produce a small flux change [i.e., drop $\partial\Phi_J/\partial t$ in (15)]; this corresponds to the low velocity or low-frequency limit, where the resistance dominates, and which gives drag only. (Nevertheless, drag is of interest by itself, as seen from the example in Sec. VIII.) The method of solution that Maxwell employs—the receding image construction—gives the response at all frequencies. That includes the high-frequency or high velocity limit, which is dominated by self-inductance effects, and leads to nearly complete shielding, as if the conductor were nearly a superconductor. Maxwell's work may have been the first instance in which high-frequency shielding was considered. In this limit the force is dominated by lift, the basis of eddy current MAGLEV.

VII. BEYOND MAXWELL'S THEORY OF EDDY CURRENTS

In this section we consider the more general problem of electromagnetic shielding by conductors, first for bulk systems, then from the viewpoint of Lenz's law, then with finite thickness effects included, and finally at frequencies so high that the displacement current must be included. Since $d \ll \delta$ for Maxwell's theory of eddy currents in thin conducting sheets to apply, the high-frequency limit discussed above for thin sheets is, in fact, only a "semihigh" frequency limit. As will be shown, in the context of eddy currents, only when $d \gg \delta$ does one reach the high-frequency limit for bulk material.

A. General analysis of eddy current shielding, lift, and drag

It is possible to extract useful information about the frequency dependence of the response using very general considerations based upon the field-diffusion equation. Consider an arbitrary conductor, of uniform dc conductivity σ, and an external current source $\mathbf{J}_s$. The current source produces a field $\mathbf{B}_s$ which, from (25) and (26), and with neglect of the displacement current term, satisfies

$$\nabla^2 \mathbf{B}_s = \mu_0 \nabla \times \mathbf{J}_s. \tag{74}$$

By (74), within the conducting material the field due to the external source satisfies

$$\nabla^2 \mathbf{B}_s = 0 \text{ (within conductor)}. \tag{75}$$

Because of this, when one decomposes the field according to

$$\mathbf{B} = \mathbf{B}_s + \mathbf{B}_J, \tag{76}$$

and then employs (74), the field-diffusion equation (34) may be rewritten as

$$\nabla^2 \mathbf{B}_J = \mu_0 \sigma \left(\frac{\partial \mathbf{B}_s}{\partial t} + \frac{\partial \mathbf{B}_J}{\partial t} \right) \text{ (within conductor)}. \tag{77}$$

This form, which is equivalent to (34), is somewhat analogous to (37), where the total time derivative effectively drives an integral of the Laplacian across the thin conducting sheet, yielding a spatial derivative rather than a Laplacian.

Let us now perform a Fourier analysis in time, so that $\partial_t \rightarrow -i\omega$. Then (77) becomes

$$\nabla^2 \mathbf{B}_J = -i\omega \mu_0 \sigma (\mathbf{B}_s + \mathbf{B}_J) \text{ (within conductor)}. \tag{78}$$

To treat the low-frequency limit, let us formally invert (78), so that

$$\mathbf{B}_J = -i\omega \mu_0 \sigma \nabla^{-2} (\mathbf{B}_s + \mathbf{B}_J). \tag{79}$$

Clearly, $\mathbf{B}_J$ is small if ω is small, so that self-induction effects are small. An expansion in $\mathbf{B}_J$ then leads to the form

$$\mathbf{B}_J = -i\omega \mu_0 \sigma \nabla^{-2} \mathbf{B}_s - (\omega \mu_0 \sigma)^2 \nabla^{-2} (\nabla^{-2} \mathbf{B}_s) + \cdots. \tag{80}$$

The first term, which is out of phase, leads to dissipative effects. Torques or forces due to this term lead to drag. Thus on very general grounds one expects that a magnet pulled across a current sheet at a low velocity will feel a drag force proportional to the velocity. The second term, which is in phase, does not lead to dissipative effects, but rather to forces pushing the conductor away from the source of the time-varying external magnetic field. Again, on very general grounds, one expects that a magnet pulled across a current sheet at a low velocity will feel a repulsive force proportional to the square of the velocity.

To treat the high-frequency limit, let us rewrite (78) in the form

$$\mathbf{B}_J = -\mathbf{B}_s + (i/\omega \mu_0 \sigma) \nabla^2 \mathbf{B}_J. \tag{81}$$

Clearly, if ω is large, then the leading term on the right-hand side of (81) is the first term, so that at high frequencies, the induced field completely cancels out the applied field. This means that self-inductance effects dominate resistive effects. Hence, the force on the conductor (and on the source) will be independent of frequency. Note, how-

ever, that one cannot successfully solve this equation by an expansion in inverse powers of ω, because if $-\mathbf{B}_s$ is substituted for $\mathbf{B}_J$ in the second term on the right-hand side of (79), (79) yields the result that $\mathbf{B}_J = 0$. This is a consequence of the fact that the frequency itself is part of what happens when the Laplacian acts on $\mathbf{B}_J$: for a large system, the characteristic length is the penetration depth (38), which depends on ω; for a small system, the characteristic length is the thickness, which is independent of ω. As a consequence, at high frequencies one must distinguish between thick and thin samples. Equivalently, for samples of a given thickness, one must distinguish between "semihigh" frequencies, where the low-frequency condition $d \ll \delta$ continues to apply, but a new condition ($v \gg v_0$ for a moving source, $\omega h \gg v_0$ for an oscillating source) is added, and high frequencies, where $d \gg \delta$. Maxwell's theory of thin conducting sheets applies only to this "semihigh" frequency regime. We will return to this question after a discussion of Lenz's law.

B. On Lenz's law

The history and "original intent" of Lenz's law, first enunciated in 1834, is of some interest, both because of what it does say, and what it does not say, about induced currents in an electrical conductor. Magie's translation of Lenz is:[21] *If a metallic conductor (e.g., a wire) moves in the neighborhood of a galvanic current or of a magnet, a galvanic current will be produced in it which will have such a direction that it would have occasioned in the wire, if it were at rest, a motion that is exactly opposite to that here given to the wire, provided that the wire when at rest is movable only in the direction of motion and in the opposite direction.* (The parenthesis has been added, for clarity.)

In Sec. 542 of his Treatise, Maxwell states Lenz's Law as:[3] *If a constant current flow in the primary circuit A, and if, by the motion of A, or of the secondary circuit B, a current is induced in B, the direction of this induced current will be such that, by its electromagnetic action on A, it tends to oppose the relative motion of the circuits.* (Maxwell also makes the interesting observation that "An earlier attempt at a statement of such a relation was given by Richie in the *Philosophical Magazine* for January of the same year, but the direction of the induced current was in each case stated wrongly.")

Whittaker gives Lenz's Law as:[20] *When a conducting circuit is moved in a magnetic field, the induced current flows in such a direction that the ponderomotive forces exerted on it tend to oppose its motion.*

Later formulations stress Lenz's law as referring to the sign relating the electromotive force and the rate of change of the flux in Faraday's law, which, according to Whittaker, was first formulated quantitatively by F. Neumann in 1848.[22] Jeans calls the relation between the induced electromotive force and the rate of change of the magnetic flux *Neumann's law* and he calls *Lenz's law* the rule that gives the sign relation in Newmann's Law.[23] Indeed, Jeans does not mention Faraday at all when he states these laws.

It is clear from the above quotations that Lenz's law was originally formulated to apply only to cases where there was relative motion of a conductor and a source of magnetic field. Indeed, at that time, the velocities obtainable were relatively low, and could not have been expected to provide effects like lift, which at low velocities are proportional to the square of the velocity. Thus the statements of Lenz's law that emphasize motion were intended to apply only to first order in the velocity, and hence only make a statement about drag forces.

Modern formulations of Lenz's law tend to emphasize the fact that the induced currents produce a field that opposes the change in the flux, rather than that they produce a force to oppose relative motion. Nevertheless, it would be useful to have a version of Lenz's law that emphasizes motion, and is general enough to include relative motion in all directions, especially when the conductor is an extended object (such as a chunk of metal), rather than a neatly defined circuit.

Such a generalization may be expressed as: *A conductor, when subjected to a time-varying magnetic field, feels a force due to induced currents, in that direction where the dissipation rate (or rate of entropy production) due to the induced currents is least.* This follows from the fact that the rate of dissipation is given by

$$\mathscr{P} = \int \frac{J^2}{\sigma} dV, \quad \mathbf{J} = \sigma(\mathbf{E} + \mathbf{v} \times \mathbf{B}) \tag{82}$$

and any change in $\mathscr{P}$ due to a change in velocity $\mathbf{v}$ is given by

$$\delta\mathscr{P} = 2 \int (\mathbf{J} \cdot \delta\mathbf{v} \times \mathbf{B}) dV = -2\mathbf{F} \cdot \delta v, \tag{83}$$

where the force

$$\mathbf{F} = \int dV \, \mathbf{J} \times \mathbf{B}. \tag{84}$$

Since, for a conductor of mass M, acted on by a force $\mathbf{F}$ for a time δt, Newton's law gives

$$\delta\mathbf{v} = \mathbf{F}\delta t / M, \tag{85}$$

the system develops a change in velocity in such a direction that $\delta\mathscr{P}$ is minimized. This is true for any velocity, and can account for the directions of forces in all three directions, as seen in our earlier discussion of a monopole above a rotating disk, where lift, drag, and a radial force were treated. Faraday's law has been implicitly invoked in the motional emf term, $\mathbf{v} \times \mathbf{B}$, which drives the current. Had the sign of this term been different, the sign of Lenz's law would also be different, in which case Lenz's law would predict that conductors are drawn into time-varying magnetic fields; of course, this is contrary to experience.

Note that a formulation of Lenz's law in terms of minimization of Joule heating permits a simple Lenz's law explanation of the dramatic Elihu Thomson jumping ring[24] and Edgerton boomer[25] demonstrations. In these cases, conductors that were initially at rest with respect to fixed field sources are violently thrust away from the region of the field when the field commences, and continues, a rapid time variation. In both cases, it is essential that the external field be nonuniform, otherwise no motion would occur (as for a magnetic dipole in a uniform magnetic field).

C. Finite thickness effects

Klauder[26] has considered the motion of an infinitely long current-carrying wire moving with a uniform velocity normal to its axis and parallel to a *semi-infinite* planar conductor. Using Fourier analysis in real space, he found the drag and lift forces for this case, particularly emphasizing

the limit where the penetration depth δ of (38) was much less than the height h of the wire above the plane. Note that for $\delta \ll d$, Maxwell's receding image technique does not apply, but the approach by Klauder does. One of the predictions is that the ratio of drag to lift in that case is proportional to $\sqrt{v_0'/v}$, where $v_0' = 2/(\mu_0 \sigma h)$. As a consequence, when v is large the power dissipation increases as $\sqrt{v}$. The physical reason for this is that the eddy currents are confined to a flow-channel of smaller area, with one of the cross-section dimensions changing from d to δ, and therefore the effective resistance of their flow-channel increases. Hence, at some point it becomes uneconomic (per unit time) to increase the velocity v in order to increase the lift force. However, per unit distance, even in this case it continues to get less expensive, because the power per unit distance goes as $v^{-1/2}$. This is the case referred to in the previous section, where it was argued that the response in the high-frequency limit depends on the sample thickness. Reitz and Davis considered the case of a current-carrying wire moving above a sheet of finite thickness, thereby obtaining results valid in both the thin and thick limits.[27] This work is of both practical and pedagogical interest.

Landau and Lifshitz[28] give a general discussion of eddy current heating, using (82) in the rest frame of the conductor, or

$$\mathcal{P} = \int \sigma E^2 \, dV. \tag{86}$$

By the discussion of Sec. VII A, at low frequencies the magnetic field is essentially the source field. Then (31) yields $|\mathbf{E}| \sim (l\omega)|\mathbf{B}_s|$, since the gradient operator in (31) yields a value on the order of $|\mathbf{E}|/l$, where l is the smaller of either the characteristic distance to the source or the characteristic dimension of the conductor. Hence, since $\mathbf{B}_s$ penetrates the sample, the rate of dissipation is proportional to ω^2 at low frequencies.

At high frequencies, $\mathbf{B}$ is non-negligible only within a penetration depth δ rather than within a characteristic depth of the conductor. Moreover, the gradient operator in (31) leads to a value on the order of $|\mathbf{E}|/\delta$ rather than $|\mathbf{E}|/l$. Hence, the dissipation rate at high frequencies includes a factor of $\delta^3 \sim \omega^{-3/2}$ that does not appear at low frequencies, so that the dissipation rate at high frequencies is proportional to $\omega^{1/2}$.

Application of these ideas to the thin conducting sheet, however, leads to a complication. There is indeed a low-frequency regime with $d \ll \delta$ where its current density $\mathbf{K}$ is proportional to ω, and its dissipation rate is proportional ω^2. However, even with $d \ll \delta$ there is an additional frequency regime where $\mathbf{K}$, since it causes complete shielding, as for a superconductor, has a pattern that is independent of frequency, and therefore the rate of dissipation is independent of frequency. We called this a "semihigh" frequency regime in Sec. VII A. For the thin conducting sheet, this regime satisfies the condition that $\omega h \gg v_0$, which is equivalent to $hd \gg \delta^2$. The $hd \gg \delta^2$ constraint is significant: if $d = 0.1h$, it is not possible to attain this regime; if $d = 0.01h$, it is possible.

We will argue that, for a thin conducting sheet of more general shape, if h is replaced by h' (the smaller of h and the characteristic transverse dimension l of the conductor), then the condition $h'd \gg \delta^2$ must be satisfied for this "semihigh" frequency shielding regime to occur. For example, it is shown in Ref. 29 that, for an oscillating magnetic field parallel to the axis of a cylinder of radius R (so $h' = l = R$) and thickness $d \ll R$, shielding occurs if this constraint holds. An alternate and equivalent view is that shielding occurs when $\omega \gg \tau_m^{-1}$, where the characteristic magnetic diffusion time τ_M is on the order of $\mu_0 \sigma R d$.[25] As is clear from both of these works, the factor of R arises from Faraday's law, giving the characteristic scale of variation of $\mathbf{E}$ along the surface, and the factor of d arises from Ampere's law, giving the scale of variation of $\mathbf{B}$ normal to the surface. Note that a diffusion equation with less complex boundary conditions than for the electromagnetic field (such as the case of thermal diffusion) would have a spectrum of diffusion times where the thickness d enters quadratically.

Our argument invokes the spectrum of magnetic diffusion times τ_M appropriate to a thin conducting sheet, which are on the order of at most $\mu_0 \sigma l d$, and consideration of the field profile due to the source, expanded within the conductor as a linear combination of eigenfunctions associated with the magnetic diffusion times. If the distance from the source to the conductor is large, so $h \gg l$, then the field profile is slowly varying in space, and a relatively few magnetic relaxation modes, with times on the order of the longest value, $\mu_0 \sigma l d$, are relevant to the electromagnetic response of the system. For frequencies much higher than the inverses of these characteristic relaxation times, the field can be expelled. On the other hand, if $h \ll l$, then the field profile is rapidly varying in space, and many more magnetic relaxation modes, with a much shorter characteristic magnetic relaxation time on the order of $\mu_0 \sigma h d$, are relevant. Nevertheless, for frequencies much higher than the inverses of these characteristic times, the field can be expelled.

We repeat that, in this $h'd \gg \delta^2$ frequency regime, the rate of dissipation is independent of frequency. Only at still higher frequencies will $d \gg \delta$, in which case the argument of Ref. 28 will apply, leading to a dissipation rate proportional to $\omega^{1/2}$.

For additional examples of frequency-dependent response, the reader is referred to the problems in Sec. 45 of Ref. 28, where a conducting sphere of radius a, and an infinitely long conducting cylinder of radius a, are subject to oscillating external fields. The $\delta \ll a$ and $\delta \gg a$ limits are considered explicitly.

We close this discussion with some brief comments on what happens at frequencies so high that either (42) or (43) is violated.

D. Extremely high-frequency effects

For a poor conductor, as the frequency increases, one must first correct the theory by including the displacement current, and then by letting the response become dominated by the inertia of the charge carriers. Including the displacement current leads to propagation even within the conductor, with energy loss due to the finite conductivity. As the frequency increases this energy loss falls off, in part because at very high frequencies the response of the charge carriers becomes dominated by their inertia.

For a good conductor, as the frequency increases, one must first correct the theory by letting the response become dominated by the inertia of the charge carriers, and then by including the displacement current. When both are included, there are two regimes. For $\tau^{-1} < \omega < \omega_p$, plasma

oscillations shield the external field with a characteristic length on the order of c/ω_p. At higher frequencies, where $\omega > \omega_p$, the charge carriers can no longer shield out the external field, and propagation occurs even within the conductor. Thus ultraviolet light penetrates a good conductor (the "ultraviolet window"), whereas infrared light is reflected.

Reference 29 discusses an interesting effect that can occur for very thin films of good conductors, where the surface is sufficiently rough that it causes the mean-free path to become on the order of the sample thickness, thus decreasing τ (and σ) enough that the system may no longer be in the category of good conductor. If that is the case, then the dc conductivity may be used along with the displacement current. This leads to surprisingly large absorption, due to interference effects, with a characteristic distance for absorption on the order of $2(c\mu_0\sigma)^{-1}$, where c is the velocity of light.

VIII. CONCLUDING EXAMPLE: DRAG ON A MAGNET FALLING DOWN A CONDUCTING TUBE

It is unfortunate that a subject as fundamental and as applicable as eddy currents has been relatively neglected in textbooks on Electromagnetism. Clearly, a few pertinent examples should be introduced to the curriculum. Certainly, the monopole creation example given in Sec. II is not a taxing one, despite the relative complexity of the derivation of the theory. Reference 7 contains the example of dipole creation, including figures of the eddy current pattern and its decay.

Surely any reader who has followed the text this far has already been convinced of the importance of the present subject. Nevertheless, we close with yet another example of the effects of eddy currents, one which, although not susceptible to the method of receding images, is a bit more realistic than the examples considered so far, since it does not require the simulation or discovery of a magnetic monopole.

The reader is encouraged to obtain a powerful rare-earth magnet (preferably neodymium–iron–boron) that will fit within a conducting tube (e.g., copper tubing for house plumbing). Dropping the magnet down the tube and watching the magnet fall at a slow, nearly constant velocity, with a gentle side-to-side motion that returns the magnet to the center, gives the observer a remarkable manifestation of the reality of eddy currents. The author has given magnet and tube to individuals ranging in age from 6 to 80, and has found that this demonstration never fails to amaze and entertain. In practice, we have employed magnets about 1/4 in. in diameter and 1/4 in. in length, and copper tubes about 3/8 in. in outer diameter, 1/32 in. in thickness, and 2 to 3 ft in length, but we suggest that the reader try the most readily available materials, and then make adjustments if the effect is not as dramatic as desired.

If the magnet is approximated as a dipole of strength m, and the tube is taken to be of infinite length, radius a, thickness d, and mass M, then the terminal velocity v_t can be obtained by a straightforward derivation. Since we know by Lenz's law that the drag force F_D must oppose the motion of the magnet, we do not take care in determining the signs in each of the steps in the derivation.

First, consider a cone with its vertex at $(0,0,z_0)$ and its base a ring of radius a, with its normal along the z axis and its center at $(0,0,z')$. By Coulomb's law for magnetic "charge" the magnetic flux produced by a monopole q^* at $(0,0,z_0)$, is given by

$$\Phi_{q^*}=\frac{\mu_0 q^*}{2}\left(1-\frac{z_0-z'}{\sqrt{a^2+(z_0-z')^2}}\right). \tag{87}$$

Second, the magnetic flux Φ of a magnetic dipole m, consisting of q^* at $(0,0,z_0)$ and $-q^*$ at $(0,0,z_0+\delta)$, where $m=q^*\delta$, can be obtained from (87) by differentiation and multiplication by δ, with the result that

$$\Phi=\frac{\mu_0 m}{2}\frac{a^2}{r_0^3},\quad r_0^2=a^2+(z_0-z')^2. \tag{88}$$

Equation (88) can be applied even if the magnet is moving along the axis, so long as its velocity v is much less than the characteristic recession velocity v_0. In that case, the total flux is essentially due to the moving magnet, with the flux due to the induced eddy currents (which we will shortly compute) being of higher order in (v/v_0), as discussed in previous sections. Thus, thirdly, if the magnet is moving downward at velocity v, by Faraday's law the emf on the ring is given by

$$\mathscr{E}=-\frac{\partial\Phi}{\partial t}=\frac{\partial\Phi}{\partial z'}v=-\frac{3\mu_0 m a^2 v}{2}\frac{(z_0-z')}{r_0^5}, \tag{89}$$

Fourth, if the ring has conductivity σ, height dz', and thickness $d\ll a$, so that its conductance is $dG=(\sigma d/2\pi a)dz'$, and if self-inductance effects are neglected, by Ohm's law this emf produces a current in the ring that is given by

$$dI=\mathscr{E}\,dG=\frac{3\mu_0 m a v\sigma d}{4\pi}\frac{(z_0-z')}{r_0^5}dz'. \tag{90}$$

Fifth, by the Biot–Savart law [e.g., Eq. (34-11) of Ref. 1] this current in the ring produces a field along the z axis at any point $(0,0,z)$, given by

$$dB_z(z)=\frac{3\mu_0^2 m a^3 v\sigma d}{8\pi}\frac{(z_0-z')}{r_0^5 r^3}dz',$$

$$r^2=a^2+(z-z')^2. \tag{91}$$

Sixth, from (91), the field-gradient, relevant to the force on the magnet, is given by

$$\frac{\partial(dB_z)}{\partial z}=\frac{9\mu_0^2 m a^3 v\sigma d}{8\pi}\frac{(z_0-z')(z-z')}{r_0^5 r^5}dz'. \tag{92}$$

Seventh, we again employ Coulomb's law for magnetic "charge," this time to obtain the drag force on the magnet at z_0: we evaluate (92) for $z=z_0$, integrate over z' from $-\infty$ to $+\infty$, and then multiply by the moment m. This yields

$$F_D=\frac{15\pi}{32}\frac{v}{v_0}F_I,\quad F_I=\frac{3\mu_0}{16\pi}\frac{m^2}{a^4}, \tag{93}$$

where F_I is the image force for a magnet at a distance a from a superconducting plane, with its moment parallel to the plane, and v_0 is Maxwell's image recession velocity, given in (1).

Finally, equating this to the pull of gravity, Mg, one obtains the terminal velocity

$$v_t=\frac{32}{15\pi}v_0\left(\frac{Mg}{F_I}\right). \tag{94}$$

In practice, one is cognizant of the fall time

$$T\approx\frac{l}{v_t}\sim\frac{m^2d}{Mga^4} \tag{95}$$

for the magnet to pass through a finite tube of length l.

From (95), an increase in permanent magnet technology (the technology of m) by a factor of 2 gives an increase by a factor of 4 in the fall time T. It was such an increase in m on going from Alnico to the rare-earths that enabled this demonstration to become so much more dramatic. Indeed, although the magnetizations of our magnets were not known, it was found that the fall time T on using Alnico magnets is far less than on using neodymium–iron–boron magnets.

Also from (95), T has an inverse fourth power dependence on the radius, and a linear dependence on σd. We have observed that, with real magnets (rather than dipoles), a slight increase in the radius a (other things being approximately the same) causes a significant decrease in T, and an increase in the thickness d (other things being approximately the same) causes an increase in T. No attempt was made at quantitative measurement.

It is worth remarking that the weaker force repelling the magnet from the side of the tube is the analog of the lift force that repels a magnet in linear motion along a thin conducting sheet. From our earlier discussion, at low velocities this force is proportional to the square of the velocity.

The emf in (89) can also be obtained by working in the frame of the magnet, and using the motional electric field $\mathbf{v}\times\mathbf{B}$. Both approaches give no induced emf normal to the conductor, and thus no surface charge density and no tendency to violate charge neutrality. However, neither of the above approaches to obtaining the current would work in the general case, where the total electric field also has an electrostatic contribution, needed in order to maintain charge neutrality. For example, there is such an electrostatic contribution for a magnet falling slowly between two vertical sheets (a case that can be obtained from Maxwell's theory, as given above, since superposition applies in the low velocity limit). Without the electrostatic contribution the current would flow only along the direction perpendicular to both the direction of motion and the normal to the plane; with the electrostatic contribution, the current flows in eddies circulating about the instantaneous position of the falling magnet.

ACKNOWLEDGMENTS

D. Ahluwalia and M. Menon were kind enough to read and make comments on early versions of the manuscript. C. Davis and T. Rossing provided useful references. M. Collins provided a number of the figures. P. Heller and C. Kittel provided encouragement and valuable suggestions. The author has three special debts: first, to C. R. Hu, for a very detailed and critical reading of the manuscript, and the suggestion to explicitly construct the gauge transformations employed to prove the vector uniqueness theorem of Appendix A; second, to J. Reitz, who suggested a number of examples considered; third, to R. M. Friedberg, who made numerous suggestions that improved the readability and the logic of the manuscript.

APPENDIX A: UNIQUENESS THEOREM FOR B USING A

It is well known that one can replace a current loop by a sheet of magnetic dipoles, so that a magnetic scalar potential formulation can be employed for current sources as well as monopole sources. The uniqueness theorem of Sec. IV would then be applicable. Nevertheless, it is often convenient to work directly with the currents, so that a direct proof of the uniqueness theorem using the vector potential $\mathbf{A}$ is desirable.

We will work with three fields and three vector potentials: $\mathbf{B}_J$ and $\mathbf{A}_J$ due to true currents (lying in the plane of the conducting sheet) developed in response to $\mathbf{B}_s$ and $\mathbf{A}_s$; $\mathbf{B}_I$ and $\mathbf{A}_I$ due to image currents developed in response to $\mathbf{B}_s$ and $\mathbf{A}_s$; and $\mathbf{B}_{I'}=\mathbf{B}_I$ with $\mathbf{A}_{I'}\neq\mathbf{A}_I$, due to the response to a gauge transformed source field $\mathbf{B}_{s'}=\mathbf{B}_s$ with an $\mathbf{A}_{s'}$ that has $A_{s'z}=0$. We will show that $\mathbf{A}_J=\mathbf{A}_{I'}$, and hence that $\mathbf{B}_J=\mathbf{B}_{I'}=\mathbf{B}_I$.

1. Vector potentials in the Coulomb gauge

In the quasistatic case, where the displacement current may be neglected, Ampere's law holds [i.e. (2)], and the current density satisfies

$$\nabla\cdot\mathbf{J}=0. \tag{A1}$$

On introducing the vector potential via

$$\mathbf{B}=\nabla\times\mathbf{A}, \tag{A2}$$

and requiring that

$$\nabla\cdot\mathbf{A}=0, \tag{A3}$$

with (5) one finds that $\mathbf{A}$ satisfies

$$\nabla^2\mathbf{A}=-\mu_0\mathbf{J}, \tag{A4}$$

with inhomogeneous solution

$$\mathbf{A}(\mathbf{r},t)=\frac{\mu_0}{4\pi}\int\frac{d\mathbf{r}\,\mathbf{J}(\mathbf{r},t)}{|\mathbf{r}-\mathbf{r}'|}. \tag{A5}$$

Note that, in time-varying situations, one may have a nonzero $\nabla\cdot\mathbf{J}$, but if the characteristic time τ_1 exceeds the relaxation time τ, the plasma oscillations have time to decay. The system then will have no bulk charge density, and thus will satisfy the $\nabla\cdot\mathbf{J}=0$ condition. Of course, it is possible to have a surface charge density, and this may move around the surface, but such effects are not large: see the end of Sec. IV C.

From (A5), it is clear that the vector potential $\mathbf{A}_J$ due to eddy currents $\mathbf{J}$ induced in a thin sheet has only two nonzero components, since its vector components are determined by the two nonzero components of $\mathbf{J}$; that is $\hat{z}\cdot\mathbf{A}_J=0$. However, for a general source, $\mathbf{A}_I\neq\mathbf{A}_J$, since the image potential for a general source will have components normal to the plane, and thus $\hat{z}\cdot\mathbf{A}_I\neq0$. Hence, the uniqueness question is not trivial. Note that, on the side opposite the source, the condition $\nabla\cdot\mathbf{J}_s=0$ guarantees that $\nabla\cdot\mathbf{A}_s=0$ and $\nabla^2\mathbf{A}_s=0$.

2. Image solution A_I in response to source A_s

Observe that, from (A5), $\mathbf{A}_J$ is even under reflection $z \to -z$ about the plane, as is B_{Jz}, but that $\mathbf{B}_{J\perp}$ is odd under $z \to -z$. The same symmetries must hold for the image field $\mathbf{B}_I$ derived from $\mathbf{A}_I$, to ensure that $\mathbf{B}_I = \mathbf{B}_J$. In computing the field on the side *opposite* to the source, all three components of the image current $\mathbf{J}_I$ must be opposite to the source current. These rules ensure that $\nabla \cdot \mathbf{J}_I = 0$, which then guarantees that $\nabla \cdot \mathbf{A}_I = 0$ and $\nabla^2 \mathbf{A}_I = 0$ on the side opposite to the source. In computing the field on the *same* side as the source, to make $\mathbf{B}_{J\perp}$ odd under $z \to -z$, the in-plane components of the source and image currents must be the same ($\mathbf{J}_{I\perp} = \mathbf{J}_{s\perp}$), but the normal components of the source and image currents must be opposite ($J_{Iz} = -J_{sz}$). These rules ensure that $\nabla \cdot \mathbf{J}_I = 0$, which then guarantees that $\nabla \cdot \mathbf{A}_I = 0$ and $\nabla^2 \mathbf{A}_I = 0$ on the same side as the source.

On the side opposite the source, in order to guarantee flux expulsion initially, and that the images recede at future times, the image solution satisfies, by analogy to (16),

$$\frac{\partial}{\partial t}(\mathbf{A}_s + \mathbf{A}_I) = -v_0 \frac{\partial}{\partial z} \mathbf{A}_I \quad (z < 0^-, z_s > 0^+). \tag{A6}$$

3. Eddy current solution A_J in response to source A_s

In (37), which was the basis for the scalar image solution, let us employ

$$\mathbf{B}_J = \nabla \times \mathbf{A}_J. \tag{A7}$$

The z component is given by

$$B_{Jz} = (\nabla_\perp \times \mathbf{A}_J)_z, \tag{A8}$$

where we have used the fact that $A_{Jz} = 0$. With (A8), (37) becomes

$$-v_0 \nabla_\perp \times \frac{\partial}{\partial z} \mathbf{A}_J = \nabla_\perp \times \frac{\partial}{\partial t}(\mathbf{A}_{s\perp} + \mathbf{A}_J) \quad (z = 0^-, z_s > 0^+). \tag{A9}$$

Hence

$$-v_0 \frac{\partial}{\partial z} \mathbf{A}_J = \frac{\partial}{\partial t}(\mathbf{A}_{s\perp} + \mathbf{A}_J) + \nabla_\perp g \quad (z = 0^-, z_s > 0^+). \tag{A10}$$

To determine g, one operates with $\nabla_\perp \cdot$ on (A10), while using the condition that, since $A_{Jz} = 0$,

$$0 = \nabla \cdot \mathbf{A}_J = \nabla_\perp \cdot \mathbf{A}_J. \tag{A11}$$

This leads to the condition

$$0 = \frac{\partial}{\partial t}(\nabla_\perp \cdot \mathbf{A}_{s\perp}) + \nabla_\perp^2 g \quad (z = 0^-, z_s > 0^+), \tag{A12}$$

which defines g uniquely, up to an irrelevant solution of the two-dimensional Laplace equation. Thus (A10) gives the boundary condition on $\mathbf{A}_J$ for $z = 0^-$. Since $\mathbf{A}_J \to 0$ as $z \to -\infty$, and since $\mathbf{A}_J$ satisfies Laplace's equation in the lower half-space, one can find a unique solution for $\mathbf{A}_J$, as in Sec. IV B where the scalar potential was considered.

4. Image solution $A_{I'}$ in response to gauge-transformed $A_{s'}$, with $A_{s'z} = 0$

Let us now make a gauge transformation on the source vector potential $\mathbf{A}_s$, so that the new vector potential $\mathbf{A}_{s'}$ has no z component. Thus introduce the scalar function f via

$$\mathbf{A}_{s'} = \mathbf{A}_s + \nabla f. \tag{A13}$$

Since the new vector potential has the property that

$$0 = \nabla \cdot \mathbf{A}'_s = \nabla_\perp \cdot \mathbf{A}'_s, \tag{A14}$$

a transverse gradient on (A13) yields

$$\nabla_\perp^2 f = \nabla_\perp \cdot \nabla f = \nabla_\perp \cdot \mathbf{A}'_s - \nabla_\perp \cdot \mathbf{A}_s = -\nabla_\perp \cdot \mathbf{A}_s. \tag{A15}$$

Taking the time derivative of (A15), and making use of (A12), yields

$$\nabla_\perp^2 \frac{\partial f}{\partial t} = -\frac{\partial}{\partial t} \nabla_\perp \cdot \mathbf{A}_s = \nabla_\perp^2 g. \tag{A16}$$

Hence, up to an irrelevant solution of the two-dimensional Laplace equation,

$$g = \frac{\partial f}{\partial t}. \tag{A17}$$

Note that, since the source fields are equal ($\mathbf{B}_{s'} = \mathbf{B}_s$), the image fields must also be equal ($\mathbf{B}_{I'} = \mathbf{B}_I$).

5. Equivalence of A_J and A_I

The response $\mathbf{A}_{I'}$ to $\mathbf{A}_{s'}$ is obtained by analogy to the case for $\mathbf{A}_J$ and $\mathbf{A}_s$. Specifically, by analogy with (A6),

$$-v_0 \frac{\partial}{\partial z} \mathbf{A}_{I'} = \frac{\partial}{\partial t}(\mathbf{A}_{s'} + \mathbf{A}_{I'}) \quad (z = 0^-, z_s > 0^+), \tag{A18}$$

where $A_{I'z} 0$ since $A_{s'z} = 0$ Substitution of (A13) for $\mathbf{A}_{s'}$ into (A18) then yields

$$\begin{aligned} -v_0 \frac{\partial}{\partial z} \mathbf{A}_{I'} &= \frac{\partial}{\partial t}(\mathbf{A}_{s\perp} + \mathbf{A}_{I'}) + \frac{\partial}{\partial t} \nabla_\perp f \\ &= \frac{\partial}{\partial t}(\mathbf{A}_{s\perp} + \mathbf{A}_{I'}) + \nabla_\perp g \quad (z = 0^-, z_s > 0^+), \end{aligned} \tag{A19}$$

where (A17) was employed in the final step. Comparison of (A10) with (A19) shows that $\mathbf{A}_J$ and $\mathbf{A}'_I$ satisfy the same equation on $z = 0^-$. Since they also satisfy the same boundary condition (zero) as $z \to -\infty$, and they both satisfy Laplace's equation for $z < 0^-$, we conclude that $\mathbf{A}_J = \mathbf{A}_{I'}$. As a consequence, $\mathbf{B}_J = \mathbf{B}_{I'} = \mathbf{B}_I$, and the equivalence of the fields $\mathbf{B}_{I'} = \mathbf{B}_I$ computed by the method of receding images, and the field $\mathbf{B}_J$ due to the true eddy currents, is finally established.

6. Additional developments

Analogously to the derivation of (17), one may show that

$$\mathbf{A}_I(x,y,z,t) = -\int_0^\infty d\tau \frac{d}{dt} \mathbf{A}_s(x,y,z - v_0\tau, t - \tau) \quad (z < 0^-, z_s > 0^+). \tag{A20}$$

Similarly, analogously to (52),

$$\mathbf{A}_I(x,y,z,t)+\mathbf{A}_s(x,y,z,t)$$
$$=v_0\frac{d}{dz}\int_0^\infty d\tau\,\mathbf{A}_s(x,y,z-v_0\tau,t-\tau)\quad(z<0^-,z_s>0^+). \tag{A21}$$

To obtain the image solution for $z > 0^+$, the same side as the source, one replaces the image at $z_s > 0^+$ by one at $z_s' = -z_s$, reflects the image motion so that $z - v_0\tau$ goes to $z+v_0\tau$, and one replaces the image $-\mathbf{A}_s$ by the image $\mathbf{A}_s'$. [The rules for image currents are that $\mathbf{J}_{I\perp}'$ is even and $\mathbf{J}_z'$ is odd, as indicated in the paragraph preceding (A6).] This construction leads, by analogy to (18), to

$$\mathbf{A}_I(x,y,z,t)$$
$$=\int_0^\infty d\tau\frac{d}{dt}\mathbf{A}_s'(x,y,z+v_0\tau,t-\tau)\quad(z>0^+,z_s'<0^-). \tag{A22}$$

Among other applications of these equations, Smythe considers the torque on a magnet rotating above a fixed, thin conducting sheet, which he remarks is relevant to the operation of a number of automobile speedometers.[2]

APPENDIX B: ADDITIONAL REFERENCES

A number of informative examples involving eddy currents are given in Chap. 10 of Haus and Melcher, a textbook written for senior electrical engineering and computer science majors.[25] For one thing, they consider a number of problems where the induced electric field is not parallel to the surface of the conductor, so that surface charge is needed to produce an electrostatic electric field to make the total field (and, thus, the electric current) parallel to the surface of the conductor. A complete solution then requires determination of the electrostatic potential, which is a significant departure from the cases considered here, where the induced electric field drives the electric current parallel to the surface of the conductor. In addition, two illustrative examples involving the transient response of cylindrical conducting sheets (shells) are given. Section 10.3 deals with the response when an axial field is turned on; Sec. 10.4 deals with the response when a transverse field is turned on. Both cases are characterized by a single magnetic diffusion time τ_M; for $t \ll \tau_M$, the shell behaves like a superconductor, "bucking out" the field, in the parlance of Ref. 25; for $t \gg \tau_M$, the field enters the shell in the steady-state configuration. The case of a thin conducting sheet is considered in one of the problems, but only the decay of a known current density is considered; Maxwell's receding image construction is not discussed. This book is filled with fresh and timely examples (stimulated by real-world applications) in the areas of electrostatics, magnetostatics, and electrodynamics.

A search of the literature available to the author at his local library revealed a number of books dealing with this subject.[30–34] None of these works seems to refer to Maxwell or to the receding image construction, although Smythe is referred to regularly.

A number of useful eddy current references deal with MAGLEV. In addition to Ref. 17, Borchert *et al.* give a general discussion of problems confronting practical application of MAGLEV.[35] Both Refs. 17 and 35 contain extensive sets of references. Borcherts and Davis consider edge and channel effects on MAGLEV.[36] Tinkham considers ac losses in superconducting magnets used for MAGLEV.[37]

With the advent of computers, it has become possible to study eddy currents numerically. A number of such studies can be found in the Proceedings of the Magnetism and Magnetic Materials Conference, published yearly in the Journal of Applied Physics, and in various of the Transactions of the IEEE. This area appears to be growing.

The author should not neglect to mention his own work on induced currents in discrete circuits. This contains a number of examples that are easily worked out for students, including the "jumping ring" and even the "sucking ring."[24]

Finally, note the paper by Pippard showing that, even in the limit of an infinite intrinsic mean-free path, a conductor cannot shield out a magnetic field forever, due to the anomalous skin-effect mechanism. In this case, the electrons that provide the shielding current—those electrons that move nearly parallel to the surface—must eventually scatter, thereby enabling their current to spread throughout the conductor.[38]

[1]David Halliday and Robert Resnick, *Physics* (Wiley, New York, 1978), third ed., part 2.

[2]William R. Smythe, *Static and Dynamic Electricity* (Hemisphere, New York, 1989), third ed., revised printing.

[3]James Clerk Maxwell, *A Treatise on Electricity and Magnetism* (Dover, New York, 1954), Vol. 2. This is an unabridged and unaltered republication of the third edition, originally published in 1891. It was edited by J. J. Thomson, the discoverer of the electron. See Chap. 12 for the "Theory of Current Sheets."

[4]James Clerk Maxwell, "On the Induction of Electric Currents in an Infinite Plane Sheet of Uniform Conductivity," Proc. R. Soc. London **XX**, 160–168 (1872).

[5]James Jeans, *The Mathematical Theory of Electricity and Magnetism*, (Cambridge U.P., Cambridge, 1960), fifth ed. (Originally published in 1925).

[6]James Jeans, "Finite Current Sheets," Proc. London Math. Soc. **XXXI**, 151–169 (1989). This work appears to be of limited applicability; moreover, in Ref. 5, Jeans remarks of this paper that "in general the results are too complicated to be of physical interest."

[7]W. M. Saslow, "How a Superconductor Levitates a Magnet, How Magnetically 'Soft' Iron Attracts a Magnet, and Eddy Currents for the Uninitiated," Am. J. Phys. **59**, 16–25 (1991).

[8]T. H. Boyer, "Penetration of the electric and magnetic velocity fields of a nonrelativistic point charge into a conducting plane," Phys. Rev. A **9**, 68–82 (1974).

[9]W. M. Saslow and G. Wilkinson, "Expulsion of Free Electronic Charge from the Interior of a Metal," Am. J. Phys. **30**, 1244–1248 (1971).

[10]I. S. Gradshteyn and I. M. Ryzhik, *Table of Integrals, Series, and Products* (Academic, New York, 1965), Eqs. (8.230). Compare with Eqs. (10.11.5) of Ref. 2, which calls the first quantity Ci, reserving the notation ci for a related quantity.

[11]J. R. Reitz, "Forces on Moving Magnets due to Eddy Currents," J. Appl. Phys. **41**, 2067–2071 (1970).

[12]"Foucault and Eddy Currents Put to Service," The Engineer **114**, 420–421 (1912), with engravings on p. 414. This article, with no byline, is on the levitation experiments and thirty-odd foot long model of an eddy-current MAGLEV train built by Emile Bachelet, of Mount Vernon, New York.

[13]J. R. Powell and G. R. Danby, "A 300-MPH Magnetically Suspended Train," Mech. Eng. **89**, 30–35 (1967).

[14]C. J. Guderjahn, S. L. Wipf, H. J. Fink, R. W. Boom, K. E. MacKenzie, D. Williams, and T. Downey, "Magnetic Suspension and Guidance for High Speed Rockets by Super-conducting Magnets," J. Appl. Phys. **40**, 2133–2140 (1969).

[15]L. C. Davis and J. R. Reitz, "Eddy Currents in Finite Conducting

Sheets," J. Appl. Phys. **42**, 4119–4127 (1971).
[16]H. T. Coffey, F. Chilton, and T. W. Barbee, "Suspension and Guidance of Vehicles by Superconducting Magnets," J. Appl. Phys. **40**, 2161 (1969) (A).
[17]P. L. Richards and M. Tinkham, "Magnetic Suspension Systems for High-speed Transportation Systems," J. Appl. Phys. **43**, 2680–2691 (1972).
[18]L. Hannakam, "Wirbelströme in dünnen leityenden Platten infolge bewegter stromdurchflossener Leiter," Elektrotech. Z. A **86**, 427–431 (1965).
[19]L. C. Davis, "Drag Force on a Magnet Moving Near a Thin Conductor," J. Appl. Phys. **43**, 4256–4257 (1972).
[20]E. T. Whittaker, *A History of the Theories of Aether and Electricity* (Dover, New York, 1989), Vol. 1. This is an unabridged and unaltered republication in one volume of the two volumes originally published by Thomas Nelson & Sons, Ltd., London, in 1951 and 1953. See p. 198.
[21]W. F. Magie, *A Source Book in Physics* (Harvard U.P., Cambridge, MA, 1963), p. 513.
[22]See pp. 199–200 of Ref. 20.
[23]See p. 453 of Ref. 5.
[24]W. M. Saslow, "Electromechanical Implications of Faraday's Law: A Problem Collection," Am. J. Phys. **55**, 986–993 (1987).
[25]H. A Haus and J. A. Melcher, *Electromagnetic Fields and Energy* (Prentice Hall, Englewood Cliffs, NJ, 1989).
[26]L. T. Klauder, "A Magnetic Field Diffusion Problem," Am. J. Phys. **37**, 323–325 (1969).
[27]J. R. Reitz and L. C. Davis, "Force on a Coil above a Conducting Slab," J. Appl. Phys. **43**, 1547–1553 (1972).
[28]L. D. Landau and E. M. Lifshitz, *Electrodynamics of Continuous Media* (Pergamon, Oxford, 1960).
[29]S. Fahy, C. Kittel, and S. G. Louie, "Electromagnetic Screening by Metals," Am. J. Phys. **56**, 989–992 (1988).
[30]J. Lameraner and M. Stafl, *Eddy Currents* (CRC, Cleveland, 1966).
[31]R. L. Stoll, *The Analysis of Eddy Currents* (Oxford, Oxford, 1974).
[32]J. A. Tegopoulos and E. E. Kriezis, *Eddy Currents in Linear Conducting Media* (Elsevier, Amsterdam, 1984).
[33]M. P. Perry, *Low Frequency Electromagnetic Design* (Dekker, New York, 1985).
[34]D. Schieber, *Electromagnetic Induction Phenomena* (Springer-Verlag, Berlin, 1980).
[35]R. H. Borcherts, L. C. Davis, J. R. Reitz, and D. F. Wilkie, "Baseline Specifications for a Magnetically Suspended High-Speed Vehicle," Proc. IEEE **61**, 569–578 (1973).
[36]R. H. Borcherts and L. C. Davis, "Force on a Coil Moving Over a Conducting Surface Including Edge and Channel Effects," J. Appl. Phys. **43**, 2418–2427 (1972).
[37]M. Tinkham, "AC Losses in Superconducting Magnet Suspensions for High-speed Transportation," J. Appl. Phys. **44**, 2385–2390 (1973).
[38]A. B. Pippard, "Lindhard's Paradox—Diffusion of Magnetic Field into a Perfect Conductor," Am. J. Phys. **58**, 1147–1152 (1990).

Hadronic numerics with quarks of *f* flavors

Wendell G. Holladay
Department of Physics and Astronomy, Vanderbilt University, Nashville, Tennessee 37235

(Received 7 October 1991; accepted 13 January 1992)

According to the "standard model" of particles and fields, hadrons can be formed from a triplet of quarks (baryons), each of which may have any one of *f* flavors (d, u, s, c, b, etc.), or from a quark–antiquark pair (mesons) each one of which may have any flavor. Some numerics of flavor and electric charge content of baryons and mesons are presented. Multiplicity of symmetry types of baryons based on these simple numerical results is calculated without direct appeal to group theory in the hope that the dimensionality of hadron multiplets that contain the building blocks of normal matter will become more widely understood.

I. INTRODUCTION

The strongly interacting particles, the hadrons (baryons and mesons), are generally classified into multiplets based on special unitary symmetry groups.[1] The associated group theory provides a powerful tool to analyze and classify hadronic properties. However, those not familiar with group theory are not enlightened by this approach and need an alternative exposition. This paper will provide such an exposition, one based on the numerics of combinations and permutations, for a few of the basic numerical features of hadronic structures. This approach depends only on simple algebraic computations and directly yields results on possible configurations of "ordinary" matter that may be more accessible to a wider audience than the approach based on the elegant but less familiar group theory.

II. QUARK CONTENT FOR BARYONS

According to the standard model of elementary particle physics,[2] the core (or valence) structure of each baryon is three quarks, each with spin $\hbar/2$ and each carrying as a seat of the strong force a different "color charge," R, G, or B, to bind the quarks together. The quarks themselves come in a number of different varieties called flavors and labeled d, u, s, c, b, and t, the first five of which have been discovered. Three of these flavors, d, s, and b, carry electric charge $-e/3$, and the other three, u, c, and t, carry $+2e/3$. Each of these flavors is characterized by a different mass.

The three core quarks in a given baryon may each have any flavor. All three quarks may each have the same flavor to yield what we call a uniflavored baryon: $\Delta^-(\mathrm{ddd})$; $\Delta^{++}(\mathrm{uuu})$; $\Omega^-(\mathrm{sss})$; etc. Two of the quarks may have the